Winter 2006

The Climate of Hays, Kansas, from 1867 to 1999: Variability, Trends, and Influences

John Heinrichs
Fort Hays State University

ort Hays Studies
Series Number 2 Spring 2006

The Climate of Hays, Kansas, from 1867 to 1999: Variability, Trends, and Influences

by

John Heinrichs

Fort Hays Studies
Fourth Series Number 2 Winter 2006

The Climate of Hays, Kansas, from 1867 to 1999: Variability, Trends, and Influences

by
John Heinrichs

Department of Geosciences
Fort Hays State University

Submitted August, 2000

Fort Hays Studies
Fourth Series, Number 2, Spring 2006

Series Editor: Bradley Will
Department of English
Fort Hays State University

Design, Layout, and Cover: Bradley Will

Support for this volume was provided by:

Tom Jackson
Dean of Graduate Studies and Research
Fort Hays State University

Larry Gould
Provost
Fort Hays State University

Fort Hays State University is a thriving liberal and applied arts, state-assisted institution with an enrollment of about 8,000 students. It offers bachelor's and master's degrees in many fields and provides a wide variety of cultural and intellectual resources, not only for its faculty, staff, and students but for the western Kansas region and beyond. Fort Hays Sate University occupies the southwest corner of Hays, Kansas, a city of about 20,000 people located halfway between Kansas City and Denver on Interstate 70. The city and its people make their livings from across a wide spectrum of industries—agriculture, education, light manufacturing, medical care, oil, retail, and technology.

Fort Hays Studies is an irregular series sponsored by the Graduate School at Fort Hays State University. The series has been published since 1939 and presents the scholarship of faculty, students, alumni, and other individuals associated with Fort Hays State University.

Dedication

This work is dedicated to Koni Steffen, who taught me how exciting and exacting climatology can be, to my parents Eugene and Beverly, who encouraged my early interest in science and love to talk about the weather, and to my wife Cheryl, without whose patience and support this research would not have been possible.

John Heinrichs
Hays, Kansas
August 8, 2000

Abstract

Hays, Kansas (38° N, 99° W), is located in a heavily agricultural area, has marginal water resources, and is subject to severe floods and droughts. Thus, quality of life in Hays is intimately tied to climate. Further, Hays is subject to a complex set of climate influences ranging from its physiography to regional circulation patterns and global climate change. In this study, records for temperature (1885 to 1999) and precipitation (1867 to 1999) were collected and examined for means, variability, ranges, trends, and periodicities. Data for a number of possible regional and global climate influences were compared with Hays climate data to characterize the relationships.

Hays has a mean annual temperature of 53.05 °F and a mean total annual precipitation of 22.78 inches. Precipitation is extremely variable over time, much more so than temperature, and relative variability is greatest in the wintertime for both temperature and precipitation. The 1930s and 1990s were abnormally warm decades, while the 1890s, 1900s, and 1910s were abnormally cool. Over the entire 114-year period, the average annual temperature of Hays has increased by about 1.7 °F, with a much faster increase over the last thirty years. Temperature in Hays has a strong year-to-year persistence, and the major cycles present in the temperature series are at 56, 11, and 3.5–4 years. The 1950s and 1930s were abnormally dry decades, and there is a noticeable 20–24-year spacing between many major flooding events. No trend was found over the 133-year period in total annual precipitation. Precipitation has very little year-to-year persistence. Major cycles present in the precipitation series are at 3.5–4 and 23 years. The analysis of possible influences on Hays climate provided a rich and complex pattern of relationships. Temperature is strongly influenced by the North Atlantic Oscillation (NAO) and Arctic Oscillation (AO) and influenced moderately by the El Niño Southern Oscillation (ENSO). Hays temperature is also related strongly to the Northern Hemispheric and global average temperatures, and this relationship is a combination of the

effects of changes in atmospheric CO_2 and solar radiation. Precipitation in Hays is strongly tied to the ENSO cycle. El Niño years are associated with increased precipitation and La Niña years with reduced precipitation. The Pacific-North American pressure pattern and Pacific Decadal Oscillation are also related to precipitation. Changes in solar radiation are related to precipitation in Hays with a lag of 5 years.

Contents

Introduction 11
Climate and Its Importance for Hays 12
Influences on the Climate and Weather of Hays 14

Methodology 23
Objectives and General Approach 23
Data Collection and Processing 23
Analysis 27

Results 29
Temperature 29
Precipitation 39

Summary and Conclusions 49
Summary of Results 49
Utility 50
Future Work 51

Acknowledgements 53

References 55

Introduction

Hays is a small city of 18,000 inhabitants located at 38° N, 99° W in the northwest part of Kansas (Figure 1). The quality of life in Hays and the surrounding region is intimately tied to climate by the importance of agriculture to the regional economy, the marginal state of local and regional water resources, and a history of destructive droughts and floods. Hays is also located in an area subject to a complex and interrelated set of climatic factors, including the variety of air masses that can affect the area,

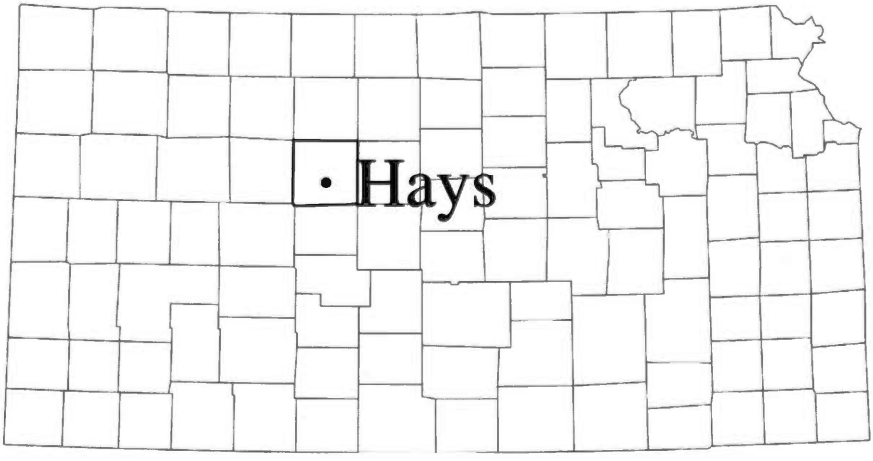

Figure 1. Map of Kansas showing the location of Ellis County (inside thicker line) and the city of Hays.

connections to atmospheric and ocean conditions in far-removed parts of the Earth, and global climate changes from natural and human causes.

Climate and Its Importance for Hays

Defining Climate

The terms climate and weather both refer to similar phenomena in the atmosphere/land system, but they differ with respect to the time scale of the phenomena. Weather is generally used to describe processes that occur over time scales of less than about 10 days (the average lifetime of a synoptic system). Climate refers to the state of the atmosphere/land system aggregated over some period of time, usually on the order of months or greater (Barry and Chorley, 1987). Climate includes the long-term mean conditions of the atmosphere and land surface as well as the variability and extremes of those conditions.

Climate and Agriculture

The importance of climate to the quality of life in and around Hays begins with agriculture. Crop production is one of the major economic activities in Ellis County, accounting for over $15 million annually in market value (USDA, 1997). Unlike many areas in western Kansas, no deep aquifer is available for irrigation, so that only 2,381 (about 1.5%) of the 155,645 harvested acres of cropland in Ellis County are irrigated (USDA, 1997). The main crops are wheat, sorghum, hay, soybeans, and alfalfa produced using dry land farming techniques. Both precipitation and temperature are critical factors determining the evapotranspiration and soil moisture and, thus, the available water for crop growth. Planning for planting and harvesting requires knowledge of the seasonal cycle of temperature and precipitation. Crop yields and the profitability of agricultural production in a given year are closely tied to the climate conditions in that year. Adams et al. (1995) and Abawi et al. (1995) have studied the impact of improved climate forecasts on agricultural producers, finding that significant benefits can be realized from accurate predictions of temperature and precipitation. Abawi et al. (1995) estimated the economic value of an accurate climate forecast at Aus$12 to Aus$20 per hectare (US$3 to US$5 per acre).

Water Resources

Another way that Hays is sensitive to climate is the marginality of its water resources. The major surface streams near Hays—Big Creek and the Smoky Hill River—do not reliably provide enough water to supply the needs of the city (P. Montoia, City of Hays Wellfield Planner, personal communication). As a result, the vast majority (95.9%) of the water for the Hays municipal water supply is extracted from ground water (Kansas Water Office, 1999). As mentioned above, Hays does not have direct access to a deep aquifer such as the Ogallala, and the bulk of the water used by Hays is drawn from a shallow unconfined aquifer, the saturated depth

of which exhibits considerable year-to-year variability (Kansas Water Office, 1999). Hurd et al. (1999), in a detailed study of the vulnerability of 240 US watersheds to changes in precipitation, ranked the watershed including Hays at the most vulnerable level in four of six supply-related indicators (natural streamflow variability, share of total precipitation that is evapotranspirated, groundwater depletion, and industrial water-use flexibility) and concluded that the region is in the uppermost rank of overall vulnerability of water supply, distribution, and consumptive use.

Floods and Droughts

Yet another impact of climate on Hays is extreme hydrologic events such as floods and droughts. Hays has several times been visited by major floods. The most destructive occurred in 1951, when a flash flood swept the city on May 22, killing six people and causing over $1.5 million in property damage (HDN, 1999). The flood was triggered by a rainfall of approximately 11 inches in 30 minutes. In 1993, a year when major flooding occurred throughout the Midwest (Chagnon, 1996), Hays again experienced flooding, and had it not been for flood protection completed after earlier floods, the city would have suffered significant damage (HDN, 1999). Other significant flooding events occurred in 1876, 1907, 1928, 1957, 1970, and 1999 (HDN, 1999). While floods in Hays are often triggered by extreme precipitation events operating over short time periods, it is important to recognize that floods are generally manifestations of climate. Precipitation falling on the land surface can travel along one of three paths: the water can reenter the atmosphere through evaporation or transpiration by plants, it can go into the soil through infiltration, or it can travel over the surface as runoff. Floods occur when more precipitation falls than can be absorbed by the soil or be carried away by the drainage network of rivers and streams. In wet years, the soil may be saturated or the streams already at high levels, so that sudden large precipitation amounts are more likely to produce flooding. Furthermore, Bell and Janowiak (1995) found that during wet years the increased soil moisture leads to greater evaporation, which increases the amount of precipitable water in the atmosphere and makes large precipitation events more likely.

Droughts have also plagued the Hays area. The worst recorded example was the Dust Bowl period in the mid- to late 1930s. During this time, soil moisture was low enough that substantial deflation and eolian removal of soil took place, although this effect was greater to the west and south of Hays (Worster, 1979). The damage to agriculture during the Dust Bowl was such that many Kansas farmers decided to leave and seek their fortunes elsewhere. During 1935, three people in the Hays area were killed directly by dust storms, including a 7-year-old boy who wandered away from his home in a dust storm and was suffocated (HDN, 1999). Another major drought from 1952 to 1956 resulted in dust storms, as did shorter droughts in 1977 and 1988. Just as with floods, droughts and associated dust

storms in Kansas must be seen as climate anomalies rather than weather events. McNab and Karl (1991) show that persistent changes in normal atmospheric circulation patterns are observed during major droughts.

Influences on the Climate and Weather of Hays

The Location of Hays

The location of Hays plays a large role in determining its climate. First, Kansas has a substantial west-to-east elevation gradient, ranging from about 4000 feet near the western border to about 700 feet in the east. It is well known that the higher in elevation a place is, generally the cooler it is (the rule of thumb is that an increase in altitude of 1000 feet corresponds to a decrease of about 3.5° F in temperature). The altitude of Hays is about 2100 feet, so it is generally cooler than places located further east and warmer than those to the west (Owenby and Ezell, 1992). Second, Hays, being located in the interior of North America, has a strongly continental climate (Barry and Chorley, 1987), which means that it is subject to a wide seasonal cycle in temperature and precipitation. Third, the Rocky Mountains lie to the west of Hays, forming a partial barrier to air flow, while no such barrier exists to the north or south. The result is that Hays is in an area into which several different air masses can move (Figure 2): mP (maritime polar) air masses can move from the Pacific Northwest bringing cool and moist weather; cT (continental tropical) air masses can bring hot and dry air from the southwest US; cP (continental polar) air masses can bring cold and dry air southwards from Canada; and mT (maritime tropical) air masses can bring warm and moist air north from the Gulf of Mexico. The mixing of these air masses can produce significant stormy weather, although the greatest amount of mixing occurs further east and south, in the part of Kansas and Oklahoma known as Tornado Alley. Finally, the Rocky Mountains modify the characteristics of air masses arriving from the west. mP air masses lose much of their moisture as they cross the Rockies, creating a partial rain shadow (Anderson, 1975). Hays is located in a precipitation region classified as Dry Subhumid (Barry and Chorley, 1987).

A major factor determining which air masses affect Hays is the large-scale atmospheric circulation, particularly the positions of the jet streams, which are high-velocity (~250 mph) upper-air westerly (i.e., west to east) wind belts. Two jets are important for Hays: the polar jet, which flows along the polar front; and the subtropical jet, which normally lies about 30° N. Changes in the positions of these two jet streams on daily to decadal time scales control the characteristics of the air over Hays, and persistent anomalous positions of the jets have been implicated in extreme weather events in the Midwest. McNab and Karl (1991) studied the 1952 drought and found that it was due to an anomalous circulation pattern in which high pressure over the Midwest and low pressure over the northeastern US resulted in more dry polar air and inhibited northward movement of moist

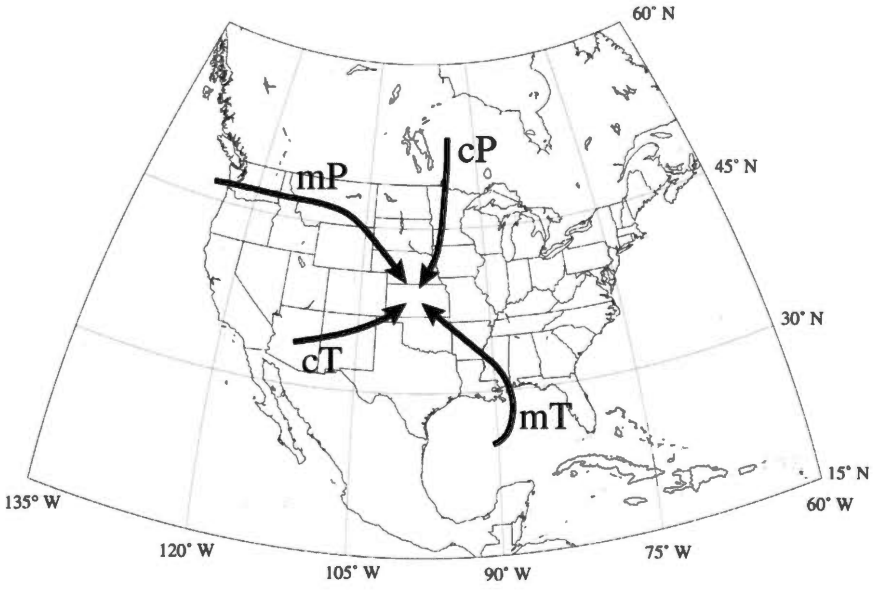

Figure 2. Types and paths of air masses that influence the climate of Hays. Abbreviations used are mP (maritime polar or cool and moist), cP (continental polar or cold and dry), cT (continental tropical or hot and dry), and mT (maritime tropical or warm and moist).

air from the Gulf of Mexico. Chagnon (1996) and Bell and Janowiak (1995) identified the position of the polar jet as a major factor in the widespread and severe flooding in 1993.

Global and Regional Climate Oscillations (Teleconnections)

One of the major revolutions in climatology over the past three decades has been the recognition that the Earth's climate system (comprising the atmosphere, oceans, lakes, rivers, flora, fauna, and land surface) has internal modes of variability (i.e., oscillations) at time scales ranging from a few years to billions of years. The shorter oscillations (i.e., those operating at time scales to years or decades) often reveal themselves as identifiable phased relationships between the climates of separate locations. The term "teleconnection" is often used to describe a relationship of this sort in which conditions in one place are associated with the same or different conditions in another place. The relevance of teleconnections to the climate of any particular location is that the observed relationships are usually most evident in the global pressure field, which drives the large-scale circulation in the atmosphere. Major manifestations of global and regional circulation patterns are the jet streams described above. Thus, the effects of many teleconnections are periodic or episodic shifts in the positions and intensities of the jet streams over North America.

The El Niño Southern Oscillation (ENSO): The ENSO was the first teleconnection to be described scientifically, and operates over global scales. The term El Niño (Spanish for "The Child") refers to an event that occurs every 3–7 years off the west coast of South America, during which the temperature of the ocean increases and the fish population decreases (associated with a decrease in ocean upwelling and the associated nutrients). The term Southern Oscillation was added when it was realized that the El Niño event represents one aspect of a much larger climate shift in which an area of warmer water (called the warm pool) migrates east from the western Pacific Ocean to the central Pacific (Trenberth, 1991). The eastwards shift of the warm pool alters the equatorial east-west (called zonal) circulation, so that the western Pacific becomes drier and the central and eastern Pacific becomes wetter. The El Niño portion of the ENSO cycle is known as the warm phase. The portion of the El Niño cycle during which the warm pool is at its western extremity is called La Niña or the cold phase. The ENSO cycle affects the climate of places far beyond the Pacific ocean, including the Sahel region of Africa, Brazil, and the Caribbean Sea (Philander, 1990). The mechanism by which El Niño affects the United States has two components. First, warmer water off the west coast promotes the formation of low-pressure systems that move onshore. Second, during El Niño years, the polar jet is weakened and moved northwards, while the subtropical jet stream is diverted to the South (Figure 3). This causes an increase in the transmission of mP (maritime polar) air masses north of the Rocky Mountains and mT (maritime tropical) air masses north from the Gulf of Mexico. Mauget and Upchurch (1999) have shown that Kansas receives a statistically significant increase in winter precipitation during an El Niño event and that wheat yields are significantly related to the ENSO cycle. Bove (1998) showed that tornadic activity in Kansas is reduced during El Niño events and increased during La Niña.

The Pacific/North American Oscillation (PNA): The Pacific/North American (PNA) pattern is characterized by a strong Aleutian low, a high pressure in the Canadian Arctic, and low pressure over the southeastern US (Philander 1990). When the PNA is in its positive phase, the polar jet stream flows in a more north-south (called meridional) orientation, bringing cold air masses from Canada to the Gulf region. When the PNA is in a negative phase, the jet stream flows in a zonal or east-west orientation (Leathers and Palecki, 1992), resulting in anomalously wet conditions in the Pacific Northwest region and dry conditions in California. The Pacific-North American (PNA) pattern has been associated with the climatic effects of the ENSO cycle over North America (Horel and Wallace 1981), although the PNA cold and warm phases do not require a corresponding shift in the ENSO cycle to occur. The possible movement of Canadian air masses southwards to the Gulf suggests that the PNA may influence the climate of Kansas and Hays.

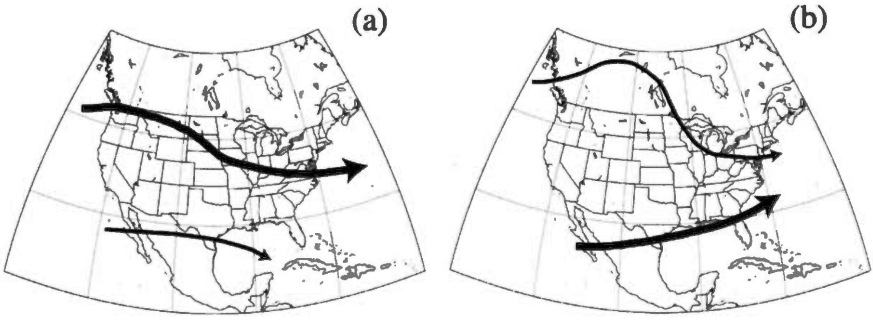

Figure 3. Positions of the polar and subtropical jet streams over North America during (a) normal and (b) El Niño conditions. The thicker line indicates a stronger jet.

The Pacific Decadal Oscillation (PDO): The Pacific Decadal Oscillation (PDO) has been identified as a distinct teleconnection more recently and operates over longer time periods than ENSO or the PNA. Scientific research on the PDO began with the observation of persistent widespread changes in the climate of the Pacific Ocean basin that occurred during the late 1970s (Trenberth and Hurrell, 1994). From the late 1970s to the late 1990s, a pool of cooler than average surface water has been located in the North Pacific, while warmer than average water has been located along the West Coast of Canada and the US (Mantua et al., 1997). Further study (Zhang et al. 1997) revealed that the late 1970s shift was only one instance of a series of interdecadal climate shifts in the Pacific. A number of effects of the PDO have been observed, including changes in the river runoff and snowpack in the Pacific Northwest and Alaska. The PDO is positively correlated with wintertime precipitation along the coast of the central Gulf of Alaska and over northern Mexico and south Florida, and negatively correlated with that over much of the interior of North America and over the Hawaiian Islands (Mantua et al., 1997). The PDO spatially behaves like the ENSO, but with a much longer period. Minobe (1997) found that the most energetic fluctuations of the PDO have had two different periodicities: 15–25 years and 50–70 years.

The North Atlantic Oscillation (NAO): The North Atlantic Oscillation has long been recognized as an important mode of variability of the atmosphere over the Atlantic Ocean (Walker and Bliss, 1932). The NAO teleconnection is a meridional (north-south) pressure shift between the north Atlantic and the central Atlantic. During what is called the positive phase of the NAO, pressures are lower than normal around Iceland (an intensified Icelandic Low) and higher than normal around the Azores and Canaries Islands (Hurrell, 1995). The negative phase involves a weaker meridional pressure gradient over the Atlantic. Positive phases of the NAO are associated with above-normal temperatures over eastern North America and changes in the jet stream over the North Atlantic (Rogers and

van Loon, 1979). The primary mechanism by which the NAO affects the United States is by varying the intensity of blocking high-pressure systems that often form off the east coast of North America. The NAO and AO are thought to be connected parts of a hemispheric pressure oscillation (Wallace, 2000), and evidence exists that the AO has been shifting over the past 40 years, possibly in response to global temperature increases (Shindell et al., 1999). Hurrell (1996), found that the NAO has undergone a dramatic change since the 1960s, which was associated with temperature changes across both major land masses in the Northern Hemisphere.

The Arctic Oscillation (AO): Another recently discovered oscillation is the Arctic Oscillation (AO), which occurs across the Arctic Basin. The positive polarity of the Arctic Oscillation is characterized by a strengthening of the polar vortex which causes cool air to move across eastern Canada, brings rain and mild temperatures to Northern Europe, and creates dry conditions over the Mediterranean region (Thompson and Wallace, 1998). During the negative phase of the Arctic Oscillation, cool continental air pushes into the Midwestern United States and Western Europe while rainfall increases in the Mediterranean.

The Quasi-Biennial Oscillation (QBO): The Quasi-Biennial Oscillation (QBO) is different from the others so far discussed in that it takes place in the upper atmosphere. It has been known for some time (Reed et al., 1961) that the zonal (east-west) winds above the equator oscillate in direction every 24–30 months (mean period 26 months). After time, the wind regimes descend in the atmosphere and begin to affect the surface flow. The QBO has some characteristics that make it a good candidate for this study. First, the phase of the QBO is known to modulate tropical cyclone activity in the Atlantic—during the east phase, the Atlantic tends to be calmer than during the west phase (Shapiro, 1989). Second, it is thought (Maruyama and Tsuneoka, 1988) that there may be a relationship between the QBO and ENSO cycles. Third, the QBO plays a role in the dispersal of dust and gases from volcanic eruptions, and the oscillation may be affected by eruptions near the equator (Maruyama, 1997).

Tropical Cyclones: One of the most important influences on the climate of the southern and eastern US is the formation of tropical cyclonic storms, including hurricanes, in the Atlantic Ocean, Caribbean Sea, and Gulf of Mexico. These storms are closely associated with the ocean surface temperature in the areas where the cyclones are formed. As discussed above, warm moist air masses originating in the Gulf of Mexico are often transported to Hays, so that the ocean temperature in the Gulf may be related to the Hays climate. In addition, tropical cyclones and hurricanes show substantial variability—some years have many storms while others have few (Landsea, 1993). The variability of tropical cyclones is related to the QBO, the atmospheric state over West Africa, and the state of the ENSO cycle (Gray et al., 1992; Gray et al., 1994; Bove et al., 1998). Strong El

Niño years tend to have reduced hurricane activity and La Niña years are associated with more hurricanes than usual.

External Forcing

Climate change: The evidence is rapidly accumulating, indeed approaching the point of certainty, that human activity is altering the climate of the entire Earth and that these changes will accelerate into the future. The primary cause for the anthropogenic changes is increasing concentrations in the atmosphere of radiatively active gases, called greenhouse gases, such as carbon dioxide (CO_2), methane (CH_4), and nitrous oxide (N_2O). These gases act to trap infrared radiation and warm the layer of the atmosphere closest to the Earth's surface (the troposphere). The increasing concentrations of greenhouse gases can be attributed largely to human activities, including fossil-fuel combustion, land-use change and agriculture. The amounts of the gases have increased substantially (by 30% for CO_2, 145% for CH_4, and 15% for N_2O) since preindustrial times (IPCC, 1995). A major reason for concern is that many of the greenhouse gases remain in the atmosphere for decades to centuries, so that warming will continue long after reduction measures are established.

Corresponding to the increased concentrations of the greenhouse gases, global average temperatures have increased by 0.3 to 0.6 °C (0.54 to 1.08 °F) since the late 1800s (Jones, 1994a), with the greatest warming taking place in the high and mid latitudes (IPCC, 1995). Observable impacts of warming include reductions in glacier mass, sea ice cover, and permafrost (Weller, 1998). Relevant to Kansas, Olsen et al. (1999), found statistically significant increasing trends in flood frequency for most parts of the Mississippi and Missouri Basins.

The concentrations of greenhouse gases in the troposphere are expected to increase to at least twice the pre-industrial levels sometime in this century. Many numerical modeling studies of the future effects on climate of the increased greenhouse gas concentrations have been performed, and a broad consensus has been reached on what can be expected. These predictions differ depending on which scenario is used for future greenhouse gas emissions. For a low-emission scenario, the global temperature increase is predicted to be about 1 °C (1.8 °F), for a high-emission scenario about 3.5 °C (6.3 °F) and for the most likely scenario about 2 °C (3.6 °F) (IPCC, 1995). The warming is expected to be greatest at high and mid-latitudes, and greater over land than over the ocean.

Hays, having a highly continental location, can be expected to warm faster than the global average. The impacts of climate change on Kansas in general or northwestern Kansas in particular have not been thoroughly assessed and cannot be completely predicted since no analog to the expected future climate has existed in historical times. However, General Circulation Model (GCM) results give some indication of what is likely to happen. A recent model-based study by Ojima et al. (1999) showed that

wintertime temperature would increase substantially over the next century (by about 7.2 °F) in the Great Plains, while precipitation would increase slightly over the same period. The increase in temperature causes a greater water loss by evaporation than is added by enhanced precipitation, so that the overall availability of soil moisture will be decreased. Enhanced convective storm activity is likely to occur, so that flooding is more likely. Using model predictions, Lettenmaier et al. (1996) found that increased monthly runoff could be expected in the Missouri Basin. It is instructive here to quote from the IPCC (1997) assessment of the impacts of climate change on North America:

> Water quantity and quality are particularly sensitive to climate change. Potential impacts include increased runoff in winter and spring and decreased soil moisture and runoff in summer. The Great Plains and prairie regions are particularly vulnerable. Projected increases in the frequency of heavy rainfall events and severe flooding also could be accompanied by an increase in the length of dry periods between rainfall events and in the frequency and/or severity of droughts in parts of North America. Water quality could suffer and would decline where minimum river flows decline. Opportunities to adapt are extensive, but their costs and possible obstacles may be limiting.

Solar Forcing: The Sun is known to exhibit variability on a number of time scales, with the most prominent cycle having a period of 11 years (Allen, 1973). The 11-year periodicity is associated with an increase in the numbers and areal coverage of sunspots and changes in the Top-Of-Atmosphere (TOA) visible flux at the Earth. Even though the flux change is small, on the order of 0.02% (Perry, 1995), insolation is the single greatest contributor to the Earth's net energy balance and the 11-year solar cycle has been observed to affect tree growth (Webb, 1986). Other cyclic variability exhibited by the Sun includes the 20–24-year Hale cycle, the 40–45-year Double Hale cycle, and the 80–90-year Gleissberg cycle (Perry, 1994). The unusually cold period between 1600 and 1750, called the Little Ice Age, is widely believed to be attributable to changes in solar output, since it was concurrent with a period of reduced numbers of sunspots (Eddy, 1976; Lassen and Friis-Christensen, 1995). Crowley (2000) studied the connections between solar output and climate over the past 1000 years and found that a substantial portion of the decadal variance of global temperature variations was due to changes in solar irradiance and volcanism. An interesting Sun-climate connection with direct relevance to Hays was found by Perry (1994, 1995), who found that precipitation lagged solar irradiance variations by 4 years in the Pacific Northwest and 5 years in the Midwestern United States. Perry (1994) attributed the lag time to the travel time of water from the Pacific Ocean to the Gulf of Alaska.

Volcanoes: The possibility that volcanoes could affect climate was first suggested by Benjamin Franklin (Sigurdsson, 1982), who observed a

particularly hard winter in the eastern U.S. after the eruption of the Laki volcano in Iceland in 1783. The powerful eruption of Tambora in Indonesia in 1815 was followed by an extremely cold winter and in 1816, which was widely known as "The Year Without a Summer," crop failures were widespread and snow fell in New England in June (Stommel and Stommel, 1983). Today the climate effects of volcanoes are universally accepted. The two major mechanisms by which volcanoes affect climate are by the ejection of dust and the release of sulfur dioxide (SO_2) from volcanic eruptions. The SO_2 combines with water in the atmosphere to form an aerosol (multitude of small droplets) of sulfuric acid (H_2SO_4). The presence of these additional substances in the atmosphere increases its optical thickness and results in a warming of the stratosphere and a cooling of the troposphere and the surface (Simarski, 1992). These effects have been observed in a number of volcanic eruptions, most notably Mt. Pinatubo in the Philippines, which erupted in June 1991. Global surface cooling reached 0.5 °C (0.9 °F) by late 1992 and returned to normal by mid-1995 (Minnis et al., 1993). Simarski (1992) found that the 1982 El Chichon eruption cooled the Earth's surface by 0.2 to 0.5 °C (0.36 to 0.9 °F).

Methodology

Objectives and General Approach

As the previous discussion shows, the climate of Hays has important consequences for the area's inhabitants and is an interesting and challenging subject for scientific study. The goal of the research described in this paper was, broadly, to develop an understanding of the long-term climate of Hays, how that climate varies at interannual to centurial time scales, and what factors at global and regional scales operate to influence the Hays climate.

The approach used for this study consisted of two major tasks, data collection and analysis. The data collection effort involved obtaining data to characterize the climate of Hays, the teleconnections, and the external forcing factors discussed above. Because many of the teleconnections and forcing factors are known to have seasonally-specific effects, monthly average data was used where available. The analysis effort began by deriving primary statistics (such as means, variability, and ranges) for precipitation and temperature. Next, the general pattern of the time series and the extreme conditions were examined. The periodicity and persistence of the climate were analyzed using autocorrelation and spectral analysis techniques, and the temperature and precipitation of Hays were examined for trends. Finally, the relationships between Hays climate and the teleconnections and forcing factors were determined using a correlation analysis.

Data Collection and Processing

Hays Climate Data

The data used in this study to characterize the climate of Hays consist of temperature and precipitation observations made at the Kansas State University Agricultural Experiment Station west of Hays (location 38°52'

N, 99°20′ W, elevation 2009.3 ft.). The temperature data consist of monthly average and annual average air temperatures from January 1885 through December of 1999. Some months of data are missing, particularly for the 1885-1888 period. The precipitation data consist of monthly and annual total precipitation (water equivalent) from January 1867 through December 1999. These data were obtained from the National Oceanic and Atmospheric Administration (NOAA) Climate Diagnostics Center (CDC) and the Kansas State Climatologist's Office.

Teleconnection Data

El Niño Southern Oscillation (ENSO): Because of the potential importance of this teleconnection on Hays climate, a number of different measures of the ENSO cycle were used in this study. First, the most common measure of the intensity and phase of the ENSO is called the Southern Oscillation Index (SOI) and is defined as the difference between the Sea Level Pressure (SLP) at Tahiti and Darwin, Australia (Figure 4). During normal or La Niña conditions, the warm water in the western Pacific leads to a lower pressure at Darwin and a positive value for the SOI. During an El Niño event, the warm water is located farther to the east, and the pressure at Tahiti is lower, so SOI values are negative. Normalized values for the SOI from 1866 to 1997, originally produced by the NOAA Climate Prediction Center (CPC), were obtained via a website operated by the Joint Institute for the Study of the Atmosphere and Oceans (JISAO) at the University of Washington at Seattle. The SOI index was calculated based on the method given by Ropelewski and Jones (1987) using early pressure sources as described by Allan et al. (1991). Second, the ENSO cycle is intimately related to Sea Surface Temperature (SST), and a frequently used measure of the strength of the ENSO cycle is the SST in the eastern pacific. The CPC has defined three regions, called NINO1+2, NINO3, and NINO4 (Figure 4), that are routinely used for analyzing ENSO. A time series of the average

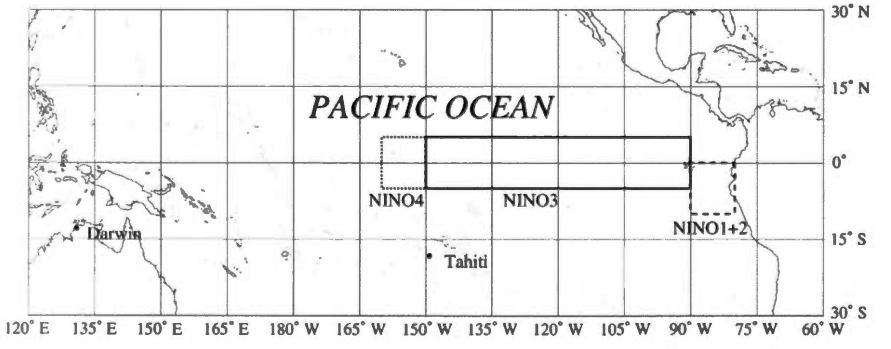

Figure 4. Location of sea surface temperature sampling regions NINO1+2, NINO3, and NINO4. The map also shows the locations of Tahiti and Darwin, which are used for the calculation of the Southern Oscillation Index (SOI).

SST over all three of these areas for the period 1950 to 1999 was obtained from the CPC website. Third, one of the manifestations of El Niño is the reversal of the normally easterly trade winds in the equatorial Pacific. Information about the direction of the equatorial winds, consisting of an ENSO zonal wind anomaly index calculated for the region 8° N to 8° S, 150° E to 140° W, was obtained for the period from 1854 to 1995 from JISAO. Fourth, a discrete measure of El Niño strength was obtained from a dataset developed by Quinn and de Mayolo (1987). Quinn and de Mayolo based their identification upon a literature search and, for the modern record, sea surface temperature observations at stations along the Peru coast (Quinn and de Mayolo, 1987; Quinn, 1992). The literature search identified such occurrences as variations in travel times between Peruvian ports, notes of unusual sea and weather conditions, presence of algae, storms, floods, and changes in marine mammal and fish populations. The dataset gives six categories of El Niño events: neutral or cold (value 0), weak moderate (1), moderate (2), strong moderate (3), strong (4), strong+ (5), and very strong (6). The Quinn data, covering a period of 1525 to 1927 were obtained from JISAO.

Pacific/North American Oscillation: The data used to characterize the PNA is the PNA index derived from a formula by Wallace and Gutzler (1981): PNA = 0.25 * [Z(20° N, 160° W) - Z(45° N, 165° W) + Z(55° N, 115° W) - Z(30° N, 85° W)], where Z are standardized 500 hPa geopotential height values. The PNA series was normalized using the standard deviation of the combined December, January, February values of 1948-97. Monthly values of the PNA Index for the 1900-Feb 2000 were obtained from the JISAO website.

The Pacific Decadal Oscillation: The variable used to characterize the PDO is the PDO index, defined as the leading principal component of North Pacific (northward of 20° N) monthly sea surface temperature anomalies normalized by the global average sea surface temperature (Mantua et al., 1997). Digital values of the PDO index were obtained for the period 1900 to February 2000 from JISAO.

North Atlantic Oscillation (NAO): The data used to characterize the state of the NAO is the monthly NAO Index based on the difference of normalized sea level pressures (SLP) between Ponta Delgada, Azores and Stykkisholmur/Reykjavik, Iceland (Hurrell 1995; Jones et al, 1997; Hurrell and van Loon, 1997). Monthly values of this index covering the period from 1865 through June 1998 were obtained from the Tiempo Cyberlibrary at East Anglia University, United Kingdom.

The Arctic Oscillation (AO): The data used to characterize the AO is the AO index described by Thompson and Wallace (1998). This index was derived using an Empirical Orthogonal Function (EOF) analysis of the pressure fields from 1958 through 1995, and then extended back to 1899 using available pressure data. Monthly values for the AO index covering

the period from January 1899 through April 1997 were obtained from the JISAO website.

The Quasi-Biennial Oscillation (QBO): The QBO index is the concatenation of the 10 hPa zonal wind (in meters per second) values at Canton Island (3° S, 172° W) for January 1953 to August 1967; Gan/Maldives (1° S, 73° E) for September 1967 to December 1975; and Singapore (1° N, 104° E) for January 1976 to February 1999 as described by Naujokat (1986) and Marquardt and Naujokat (1997). Monthly values of the QBO index for the January 1953 to February 1999 period were obtained from the JISAO.

Tropical Storms: Three related datasets were used to characterize the intensity of Atlantic tropical-storm activity. They are the total number of tropical storms in a given year, the number of named hurricanes in that year, and an index called Net Tropical Cyclones (NTC). The NTC index was developed by William Gray and his associates at Colorado State University (Gray et al., 1994) and takes into account the total numbers of tropical storms and hurricanes, the numbers of days each kind of storm last, the total number of intense hurricanes, and the number of days they last (Landsea, 1993). All of these indicators are normalized to a percentage and then averaged to produce an integrated index showing total storm activity as a percentage of normal (i.e., a value of 100 indicates an average year). The data for the tropical storm counts and indices covering the period 1950 to 1996 were obtained from a website operated by the Hurricane Research Division of NOAA's Atlantic Oceanographic & Meteorological Laboratory.

External Forcing Data

Solar Forcing: Two sources of data on solar behavior were used. The first is the monthly mean sunspot number, a measure of the number of discrete sunspot groups visible on the face of the Sun. Monthly average sunspot numbers from 1700 through May 2000 were obtained from a website operated by the International Sunspot Data Center in Brussels. The second dataset consists of estimates of the Top-Of-Atmosphere (TOA) solar flux in Watts/m^2 integrated over the entire Earth. These values were estimated using sunspot numbers before 1874, and from 1874 on using actual irradiance measurements (Lean et al., 1995). Annual values for the flux for the 1600 to 1994 period were obtained from a website operated by the NOAA Climate Monitoring and Diagnostics Laboratory (CMDL).

Global Warming: Three datasets were used as proxies for global climate change. The first two are the Northern Hemisphere and global average annual temperature time series produced as described by Jones et al. (1986) and Jones (1994b). The accuracy of this data set since 1951 is estimated at 0.05 °C or 0.09 °F (Jones et al., 1997). Values for these data sets covering the period from 1856 to 1998 were obtained from the Tiempo Cyberlibrary. The third variable is a measure of the radiative impact of CO_2 derived by Hansen et al. (1997) and updated to 1998. The CO_2 forcing

values were obtained from the NOAA Paleoclimatology Program Home Page and cover the period from 1000 to 1998.

Volcanoes: The dataset used to identify major volcanic eruptions for this study is the Volcanic Explosivity Index (VEI) defined by Newhall and Self (1982). The VEI categorizes eruptions on a scale from 1 (the lowest) to 8 (the highest) by a combination of quantitative and qualitative indicators such as the volume of ejecta, the eruption column height, the duration, and the types of eruptive products. Using this scale, the Mt. St. Helens eruption in 1980 is given a VEI of 5 while the 1815 Tambora eruption has a VEI of 7. Data covering the period 1500 to 1982 for eruptions with a VEI of 4 or greater was taken from a table in Newhall and Self (1982).

Processing

The processing performed for all of the datasets involved two basic steps. The first step was to eliminate any data occurring before 1867 or after December 1999. Partial years were also eliminated. The second step was to average the data over appropriate periods for analysis. Multiple averaging periods for some variables were used where previous studies had indicated a phenomenological reason for using a subannual period, such as a teleconnection that is active during only part of the year. For the SOI and the other ENSO related time series, December to February (Hurrell, 1996) and June to November (Redmond and Koch, 1991) averaging periods were used. For the NAO, annual averages were used following Barnston and Livezey (1987), and a wintertime (December to February) average was used as described by Hurrell (1995). Following Thompson and Wallace (1998), the AO was averaged over the December to February period and over the entire year. The PNA was averaged over the entire year and over the November to February period, since the PNA was identified by Wallace and Gutzler (1981) as being one of the two major global modes of variability during that period. Annual averages were used for all other forcing factors.

Analysis

The primary statistics for temperature and humidity—the mean and variance over the period of record—were calculated on an annual and monthly basis (averages for temperature and totals for precipitation). Because the annual cycle of temperature and pressure is so large, the coefficient of variation (the standard deviation divided by the mean) was also employed to characterize variability. Use of the coefficient of variation eliminates high apparent variability which may arise from a large magnitude range in the values of a sample population. The maximum and minimum monthly values were also identified, and a range calculated to serve as a robust indicator of variability. For both the temperature and precipitation datasets, periodicity in the data was analyzed by performing spectral and autocorrelation analyses. In the spectral analysis, a Fourier power spectrum was obtained from the raw data using a Fast Fourier Transform (FFT). The

derived power spectrum gives the amount of power contributed by periodic components (pure sine waves) of various frequencies. In the autocorrelation analysis, a correlation was calculated between the time series and itself with varying lag times. In order to determine whether trends exist in the records, the temperature and precipitation data were regressed against time, and the slopes and correlations were calculated. In addition, an f-statistic and f-test threshold (using a two-tailed heteroscedastic f-test) were calculated for each regression to evaluate the significance of any observed trends. A 95% significance level was used to eliminate all but the most certain trends. The significance level represents the probability that the observed relationship is real and not merely an artifact of the random choice of values for the population.

The relationships, between the forcing variables and the Hays temperature and precipitation data, were analyzed by regressing the forcing variables against the Hays time series. Two runs were made for each forcing variable—one to examine the relationship between the forcing variable and the Hays climate in the same year and another to examine the relationship between the forcing variable and Hays climate in the following year. This is important because some of the teleconnections have a built-in lag as their effects travel over regional and perhaps global scales. F-tests at the 95% significance level were conducted for all regressions. No attempt was made so separate collinearity between the forcing variables such as the interaction between the NAO and the AO. For discrete forcing variables, such as the Quinn El Niño time series, the average temperature and precipitation for specified values of the forcing variable was calculated and compared to the average of all years. A Student's t-test was applied to determine the probability that the means of the selected and entire populations are the same. Since the time periods covered by the data for the forcing factors differed widely, two separate analyses were performed—one using the full periods of record for all variables and the other using only the 1953 to 1994 period, for which data was available for all variables. The first analysis makes full use of the data and illustrates the patterns present over the longest possible time period, while the second allows the magnitudes of the relationships to be compared with each other directly.

Results

Temperature

Means and Variability

Table 1 shows the basic statistical parameters for the 1885 to 1999 Hays temperature record. The minimum monthly average temperature occurs in January and the maximum monthly average temperature occurs in July. The large difference between the seasonal temperature extremes (50.91 °F) is typical of a continental climate. The increase in temperature through the first half of the year is more rapid than the decrease in the second half. The variability of temperature in Hays is clearly greatest during the winter and early spring months in both absolute and relative senses. The standard deviation is greater in January, February, and March; the coefficient of variation is greater in December, January, and February; and the range is greater in January, February, and March.

TABLE 1
Overall statistical parameters for the Hays temperature time series (1885 to 1999) on monthly and annual bases.

	JAN	FEB	MAR	APR	MAY	JUN	JUL	AUG	SEP	OCT	NOV	DEC	TOT
Average (°F)	27.31	31.70	41.14	52.78	62.14	72.35	78.22	76.64	67.58	55.37	40.57	30.84	53.05
Std. Dev. (°F)	5.40	5.85	5.08	3.33	3.14	3.50	3.17	3.09	3.09	3.19	3.20	4.48	1.48
Coeff. of Variation	0.20	0.18	0.12	0.06	0.05	0.05	0.04	0.04	0.05	0.06	0.08	0.15	0.03
Min. (°F)	12.07	17.49	27.04	43.97	55.09	63.73	70.49	68.95	60.96	45.41	32.13	14.46	49.27
Max. (°F)	37.77	44.46	52.45	60.79	69.60	81.10	86.26	84.45	77.28	65.37	48.60	42.93	56.55
Range (°F)	25.70	26.97	25.41	16.82	14.51	17.37	15.77	15.50	16.32	19.96	16.47	28.47	7.28

Time Series Analysis

Extremes: Table 2 shows the 20 warmest years and 20 coldest years during the 1885 to 1999 period. An immediate observation is that 5 of the 20 warmest years occurred during the 1930s. This compares with the 1.75 that would be expected in a randomly chosen sample of 20 years. A chi-square test shows that the probability of such a large number of years from a single decade in the top 20 is 0.0103, so we can conclude that the 1930s were abnormally warm with a significance level of 95%. Four of the 20 warmest years fell in the decade of the 1990s, compared with 1.75 that would be expected for a uniform distribution. A chi-square test shows that the probability of this occurring due to randomness is 0.0758, so the 1990s can be said to be warmer than the norm at the 90% significance level. Illustrating the warmth of these decades is the fact that not a single year from the 1930s or 1990s appears in the list of the twenty coldest years.

A similar analysis shows that the decades of the 1890s, 1900s, and 1910s, each with 4 of the 20 coldest years, were abnormally cold with a significance

TABLE 2
The 20 warmest and 20 coldest years in Hays during the 1885 to 1999 period.

The 20 Warmest Years		The 20 Coldest Years	
Year	Average Annual Temperature (°F)	Year	Average Annual Temperature (°F)
1934	56.55	1895	49.27
1946	56.35	1903	50.20
1954	56.13	1912	50.61
1933	55.96	1951	50.64
1938	55.86	1892	50.75
1986	55.80	1993	50.85
1939	55.76	1929	51.06
1998	55.70	1904	51.08
1991	55.61	1905	51.12
1963	55.40	1924	51.13
1999	55.40	1898	51.26
1987	55.31	1960	51.28
1921	55.26	1915	51.42
1953	55.13	1985	51.44
1990	54.99	1961	51.58
1931	54.98	1917	51.64
1981	54.96	1909	51.65
1988	54.93	1893	51.66
1977	54.90	1979	51.66
1994	54.68	1919	51.69

level of 90%. These conclusions are confirmed by an examination of Figure 5, which shows temperature referenced to the long-term mean and an 11-year moving average of temperature. The particular average used is called a "boxcar" average and aggregates each year with the 5 years preceding and 5 years following it. The 11-year period for the moving average was chosen in order to reveal the long-term temperature variation and eliminate any short-term variability from such sources such as teleconnections or solar forcing. In Figure 5, the contrast between the colder period from 1885 to about 1920 and the warmer period from 1920 to about 1960 is obvious, as is the extreme warmth of the 1930s. The period from 1960 until about 1978 was cooler than average, and the recent period, particularly the 1990s, has higher than normal temperatures.

Trends: The regression of average annual temperature against time over the period of record (Figure 6) shows that there has been a substantial increase of temperature in Hays since 1885. The overall increase has been about 1.7 °F (an increase rate of 0.015 °F/yr), and the trend is significant at the 95% level. The correlation of temperature with time was found to

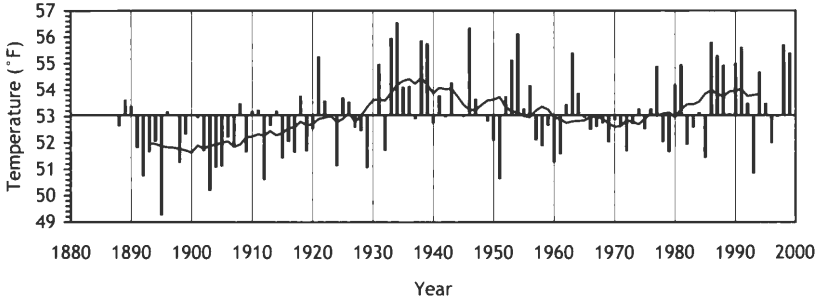

Figure 5. Annual average temperature in Hays from 1885 to 1999 referenced to the long-term mean temperature (bars) and 11-year moving average (solid line).

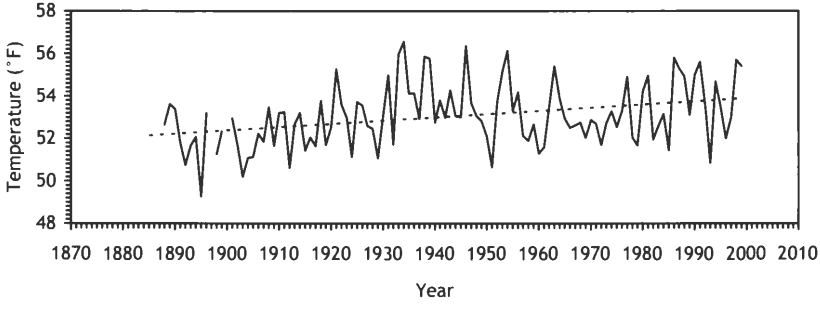

Figure 6. Annual average temperature in Hays from 1885 to 1999 (solid line) and fitted regression lines for the 1885 to 1999 period (dashed line).

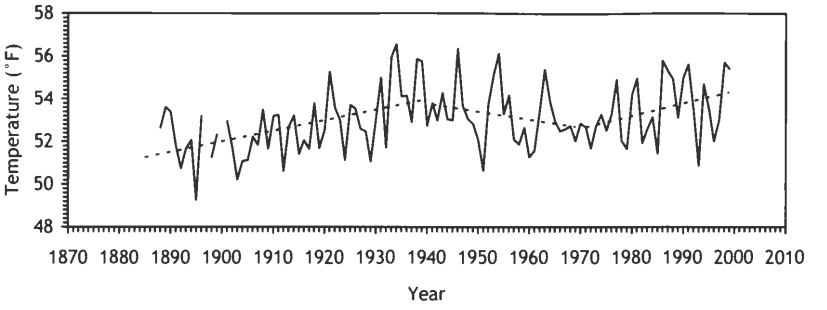

Figure 7. Annual average temperature in Hays from 1885 to 1999 (solid line) and fitted regression lines for the 1885 to 1940, 1940 to 1970, and 1971 to 1999 periods (dashed lines).

be 0.33, indicating that about 11% of the variance of the temperature time series is due to the long-term trend. The observation above of distinct temperature periods in the record suggests that processes of change have been underway. To examine this hypothesis, the temperature time series was divided into three periods (1885 to 1940, 1941 to 1970, and 1971 to 1999) that show apparent trends in Figure 7. A regression analysis was performed on each of these three periods, showing that the trends are 0.051 °F/yr, -0.036 °F/yr, and 0.057 °F/yr, respectively. Only the first of these trends is significant at the 95% level (a correlation of 0.51). However, the recent (1971 to 1999) trend is significant at the 90% level (a correlation of 0.33) and represents the greatest rate of change of temperature of the three periods (almost six-tenths of a degree per decade or about four times as fast as the overall trend).

The analysis of temperature trends by month (Table 3) shows that all months but April had an increasing trend over the period of record. The observed trends in February, June, July, and October are all significant at the 95% level. The trend for February is quite large, indicating that Februaries today are on average about 5 °F warmer than in 1885.

Periodicity: The autocorrelation analysis (Figure 8) shows that the greatest correlation (0.3) of the temperature time series with itself occurs with a lag of one year. This indicates a fairly strong year-to-year persistence of temperature—for any year, the year most like it in the record is the one immediately preceding it. The persistence of temperature in Hays at a 2-year lag, on the other hand, has a correlation very close to zero. A particularly interesting result of the autocorrelation analysis is the relatively strong negative anticorrelation (approximately -0.25) with a lag of 30 years. This is most likely related to the distinct temperature trend regimes noted earlier with lengths of about 30 years. Other lags with important correlations are 8, 10, 53, and 56 years (positive correlations) and 26, 29, 19, 39, and 31 years (negative correlations). Finally, note that the 10-year lag produces a

Table 3
Trend analysis for Hays temperature from 1885 to 1999.
Boldface indicates the trend is significant at the 95% level.

Month	Trend (°F/yr)	R	R2
JAN	0.0208	0.1244	0.0155
FEB	**0.0472**	**0.2598**	**0.0675**
MAR	0.0096	0.0611	0.0037
APR	-0.0070	-0.0678	0.0046
MAY	0.0103	0.1054	0.0111
JUN	**0.0217**	**0.1997**	**0.0399**
JUL	**0.0222**	**0.2260**	**0.0511**
AUG	0.0115	0.1198	0.0144
SEP	0.0046	0.0483	0.0023
OCT	**0.0191**	**0.1929**	**0.0372**
NOV	0.0109	0.1100	0.0121
DEC	0.0120	0.0865	0.0075
TOT	**0.0153**	**0.3324**	**0.1105**

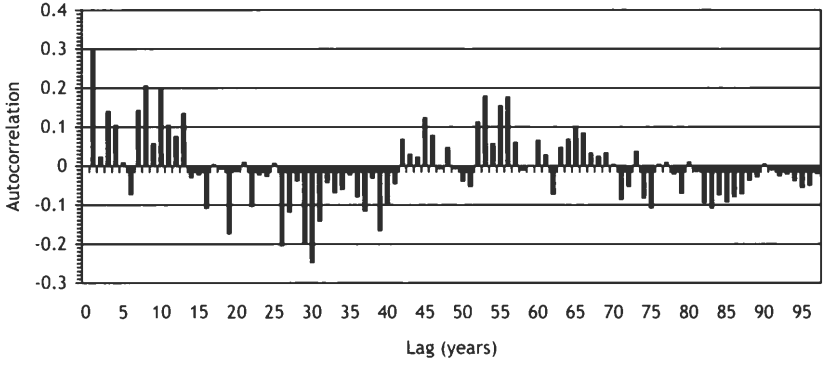

Figure 8. Autocorrelation analysis of the Hays annual average temperature time series (1888 to 1999). The vertical axis shows the correlation of the time series with itself at the lag times given on the horizontal axis.

relatively large positive correlation, possibly associated with the 11-year solar cycle.

Figure 9 shows the results of the spectral analysis of the Hays temperature time series. Spectral analysis requires a continuous time series, so missing values precluded using the 1885 to 1888 portion of the temperature dataset. Interpolated values were used for two months: March 1897 and March 1900. A Fourier spectral analysis cannot resolve contributions with wavelengths shorter than twice the sampling interval

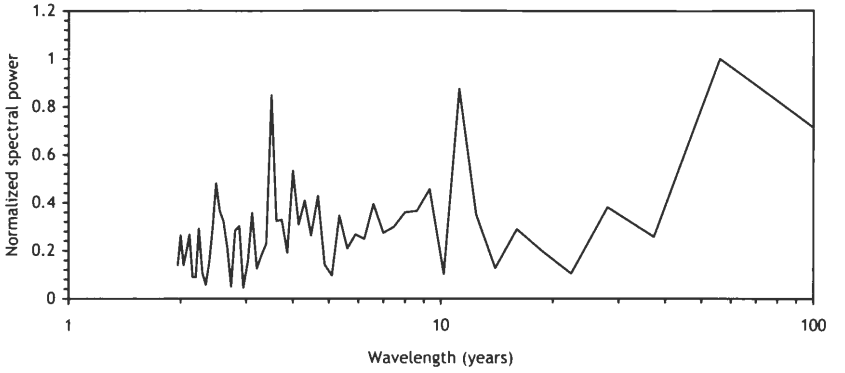

Figure 9. Spectral analysis of the Hays annual average temperature time series (1888 to 1999). The curve represents the relative importance of pure sine wave components having the wavelengths on the horizontal axis.

(Körner, 1989), so no component with a wavelength shorter than 2 years is included in the graph. The spectral analysis shows several important periodicities, including (in order of their contribution) 56, 11, 3.5, 4, and 2.6 years. The 56-year peak, which contributes the most to the temperature time series, is most likely related to the 30-year trend regimes. The 11-year periodicity strongly implies that solar variability is important to Hays temperature, while the 3.5- and 4-year peaks suggests a contribution by the ENSO cycle. The 2.6-year peak may be related to the QBO, with its period of 24–30 months. Note that none of the components near 2 years shows an important contribution. This reflects the observation above that temperature in Hays is relatively persistent from year to year so that periodicity on a 2-year time scale is relatively insignificant.

Influences on Temperature: 1885 to 1999

Table 4 shows that a very complex pattern of relationships exists between temperature in Hays and forcing factors.

ENSO: A relationship between the ENSO cycle and Hays temperature exists, but it is somewhat ambiguous. No significant correlation was found between the SOI annual or seasonal temperature. However, a moderate negative correlation exists between the June to November SST in NINO1+2 and springtime temperature in the same year. Perhaps high ocean temperatures off the west coast of South America, which are characteristic of El Niño, would be associated with increased cloudiness over Kansas and lower temperatures. Somewhat confusing the issue are moderate positive correlations (0.34 to 0.38) between two of the SST variables and temperatures in summer of the following year. These correlations may show a greater relationship to global warming than to ENSO, since SSTs have been rising generally. The Equatorial Wind variable shows no significant relationship to

TABLE 4

Correlation analysis for possible influences on Hays temperature using full periods of record. Boldface indicates relationships that are significant at the 95% level. Unless otherwise noted, the variable is averaged over the entire year. For influences that cross the end of the year, the same-year values are for the year in which the earlier part of the averaging period falls.

	Correlation to Same-Year Temperature					Correlation to Next-Year Temperature				
Variable	**Annual**	**JFM**	**AMJ**	**JAS**	**OND**	**Annual**	**JFM**	**AMJ**	**JAS**	**OND**
SOI (Jun-Nov)	-0.03	0.04	-0.14	-0.02	0.06	0.01	0.04	0.09	-0.13	0.02
SOI (Dec-Feb)	-0.10	-0.03	-0.16	-0.06	0.00	0.01	0.01	0.13	-0.16	0.05
NINO1+2 (Jun-Nov)	-0.12	0.04	**-0.36**	0.05	-0.12	0.16	0.02	-0.01	**0.34**	0.09
NINO1+2 (Dec-Feb)	-0.14	-0.06	-0.16	-0.05	-0.09	0.08	0.10	-0.15	0.27	-0.06
NINO3 (Jun-Nov)	-0.06	0.08	-0.17	-0.06	-0.08	0.26	0.14	0.01	**0.39**	0.06
NINO3 (Dec-Feb)	-0.04	0.04	-0.09	-0.06	-0.05	0.15	0.10	-0.13	**0.37**	0.00
NINO4 (Jun-Nov)	0.03	0.14	0.00	-0.08	-0.08	0.22	0.14	0.06	0.26	0.03
NINO4 (Dec-Feb)	-0.05	0.02	0.05	-0.16	-0.06	0.15	0.11	-0.08	0.27	0.02
Eq. wind (Jun-Nov)	0.07	0.17	0.06	-0.07	-0.07	0.15	0.12	0.04	0.25	-0.08
Eq. wind (Dec-Feb)	0.22	0.16	0.28	-0.08	0.13	0.19	0.07	0.11	0.24	0.04
PNA	0.14	0.17	-0.21	0.24	0.03	0.02	-0.05	0.08	-0.01	0.07
PNA (Nov-Feb)	0.06	0.08	-0.07	0.17	-0.11	**0.33**	0.27	0.09	**0.35**	-0.05
PDO	0.07	0.03	-0.04	**0.20**	0.00	0.02	-0.10	0.08	0.13	-0.01
NAO	**0.28**	**0.35**	0.01	0.12	0.07	0.07	0.12	-0.17	**0.21**	-0.03
NAO (Dec-Feb)	-0.14	-0.06	-0.08	-0.11	-0.05	0.04	**0.30**	**-0.20**	-0.10	-0.05
AO	**0.25**	**0.32**	0.12	0.00	0.02	0.09	0.09	0.01	0.04	0.05
AO (Dec-Feb)	0.00	-0.04	0.10	-0.08	0.03	-0.04	0.18	-0.12	-0.15	-0.15
QBO	-0.11	-0.02	-0.27	0.14	-0.15	0.20	0.10	**0.31**	-0.12	0.17
Gray Storm Count	0.03	-0.04	-0.06	0.08	0.10	-0.03	-0.09	0.25	-0.11	-0.08
Gray Hurricane Count	-0.07	-0.05	-0.09	0.04	-0.04	0.03	-0.01	0.25	-0.06	-0.09
Gray NTC	-0.15	-0.11	-0.12	-0.06	-0.03	-0.09	-0.10	0.14	-0.20	0.00
Global Average Temp.	**0.39**	**0.26**	**0.15**	**0.26**	**0.22**	**0.36**	**0.27**	0.13	**0.22**	**0.19**
NH Average Temp.	**0.46**	**0.28**	**0.19**	**0.32**	**0.30**	**0.37**	**0.24**	0.12	**0.26**	**0.23**
CO2 Radiative Forcing	**0.24**	**0.25**	0.08	0.09	0.10	**0.25**	**0.24**	0.08	0.08	0.10
Lean Solar Forcing	**0.24**	0.12	0.08	0.17	**0.20**	**0.23**	0.14	0.07	0.13	0.16
Sunspot Number	-0.04	-0.11	-0.07	0.03	0.11	-0.06	-0.06	-0.09	-0.04	0.04

temperature. Table 5 shows the seasonal and annual average temperatures for the El Niño years as defined in the Quinn and de Mayolo (1987) dataset. The El Niño years are slightly cooler than the long-term average, and the difference is greater in spring and autumn than the other two seasons. However, none of these means are different from the long-term mean of all years at the 95% significance level.

PNA: The wintertime PNA index shows a fairly strong positive relationship to Hays annual average and summer temperature in the following year. A possible explanation is that when the PNA is in its positive phase and the polar jet stream is more meridional, high pressure is more likely to dominate the Hays area in summer and increase temperatures.

PDO: A weak, but significant, positive correlation exists between the PDO and same-year summertime temperature.

NAO: The NAO shows a clear relationship to Hays temperature on both annual and seasonal bases. The annual average NAO index is positively correlated to the same-year average and winter temperature and weakly positively correlated to summertime temperature in the following year. The positive phase of the NAO, in which the Icelandic Low is intensified, is associated with higher temperatures in Hays. The winter NAO index shows a somewhat different pattern, being positively correlated to winter temperature and weakly negatively correlated to springtime temperature.

AO: The annual average Arctic Oscillation index shows a similar pattern to the annual average NAO index, with slightly lower correlations. This is not surprising, considering the close relationship between the AO and NAO, and illustrates the sensitivity of Hays climate to processes in distant locations.

Tropical cyclones: The various measures of Atlantic and Caribbean cyclone activity show no significant relationships to Hays temperature in the same or next year.

Global and hemispheric temperature: This relationship is the strongest of any observed for the temperature time series. Strong positive correlations exist between both global and Northern Hemisphere temperature and annual temperature in both the same and following years. Weaker relationships exist to temperature in all seasons except spring (again in both the same and following years). The most likely explanation is that

TABLE 5
Average annual and seasonal average temperature for all years, El Niño years, and the years following El Niño years.

	Average Annual Temperature (°F)				
Years	JFM	AMJ	JAS	OND	Annual
All years	33.26	62.50	74.15	42.24	53.05
El Niño	32.21	61.94	74.31	41.64	52.48
El Niño + 1	32.80	62.19	74.25	42.62	52.94

Hays, being very continental, is tied to processes acting across the entire hemisphere and globe. An alternative explanation for this relationship is that the global and hemispheric temperature measurements are biased in favor of populated land areas where the majority of historical climate observations have been made. However, the Jones (1994b) dataset has been conditioned to remove such biases as measurement location.

CO_2 radiative forcing: This variable shows a significant relationship to Hays annual average and winter temperatures in both the same and succeeding years. The seasonal correlation pattern is similar to, but weaker than, the relationship with global and hemispheric temperatures. The consistency of these correlations suggests that warming by greenhouse gases has had some impact on the Hays climate.

Solar forcing: The Lean forcing flux data has a significant positive correlation to Hays annual average temperature, with the strongest seasonal relationship in the autumn. The magnitude of the correlations is approximately equal to that of the CO_2 radiative forcing. The sunspot-number time series has no significant relationship to Hays temperature.

Volcanoes: The volcano analysis (Table 6) shows that Hays is not strongly impacted by major eruptions. The 4 years following all 9 major eruptions during the temperature period of record are statistically indistinguishable from the overall set of years included.

TABLE 6
Average monthly and annual temperatures in Hays
in the year of and the 4 years following a major volcanic eruption.
None of these values are significantly different from the expected values at the 95% level.

	JAN	FEB	MAR	APR	MAY	JUN	JUL	AUG	SEP	OCT	NOV	DEC	TOT
Year 0	27.04	31.52	41.19	52.84	62.27	72.38	78.18	76.63	67.64	55.37	40.53	30.76	53.05
Year +1	25.64	31.64	43.12	51.95	63.45	73.47	79.52	77.31	68.18	56.28	39.45	29.73	53.31
Year +2	30.02	32.54	41.01	52.70	61.35	70.49	78.54	75.87	67.29	55.12	41.02	30.45	53.03
Year +3	27.46	29.25	37.99	51.20	63.23	71.34	78.12	77.34	65.75	55.28	42.56	30.77	52.52
Year +4	26.95	28.72	45.69	51.37	61.04	72.70	78.43	77.50	67.99	54.73	40.29	28.60	52.83

TABLE 7

Correlation analysis for possible influences on Hays temperature during the 1953 to 1994 period. Boldface indicates relationships that are significant at the 95% level. Unless otherwise noted, the variable is averaged over the entire year. For influences that cross the end of the year, the same-year values are for the year in which the earlier part of the averaging period falls.

	Correlation to Same-Year Temperature					Correlation to Next-Year Temperature				
Variable	**Annual**	**JFM**	**AMJ**	**JAS**	**OND**	**Annual**	**JFM**	**AMJ**	**JAS**	**OND**
SOI (Jun-Nov)	0.01	-0.09	0.00	0.10	0.08	-0.03	-0.01	0.07	-0.30	0.18
SOI (Dec-Feb)	-0.06	-0.07	-0.10	0.05	0.02	0.02	-0.06	0.20	-0.25	0.24
NINO1+2 (Jun-Nov)	-0.14	0.03	**-0.33**	0.03	-0.17	0.00	-0.01	-0.21	0.23	-0.03
NINO1+2 (Dec-Feb)	-0.18	-0.11	-0.09	-0.08	-0.13	-0.12	0.06	-0.30	0.14	-0.28
NINO3 (Jun-Nov)	-0.02	0.09	-0.10	-0.06	-0.06	0.12	0.12	-0.11	0.29	-0.09
NINO3 (Dec-Feb)	-0.01	0.03	-0.01	-0.04	-0.03	0.00	0.06	-0.24	0.28	-0.15
NINO4 (Jun-Nov)	0.04	0.15	0.03	-0.13	-0.07	0.09	0.09	0.01	0.16	-0.10
NINO4 (Dec-Feb)	-0.03	0.04	0.07	-0.19	-0.01	0.03	0.05	-0.11	0.18	-0.09
Eq. Wind (Jun-Nov)	0.08	0.17	0.06	-0.09	-0.06	0.10	0.10	-0.02	0.22	-0.11
Eq. Wind (Dec-Feb)	0.21	0.17	0.28	-0.12	0.13	0.17	0.07	0.08	0.21	0.04
PNA	0.15	0.10	-0.10	0.23	0.07	0.00	-0.10	0.04	-0.01	0.13
PNA (Nov-Feb)	-0.02	-0.04	-0.04	0.13	-0.09	**0.32**	0.23	0.15	0.31	-0.02
PDO	0.05	0.13	-0.10	0.06	-0.07	0.03	-0.06	0.11	0.07	0.01
NAO	0.20	**0.40**	-0.09	-0.05	-0.06	0.04	0.09	-0.13	0.19	-0.13
NAO (Dec-Feb)	-0.07	0.04	-0.19	-0.03	-0.04	-0.02	**0.39**	**-0.38**	-0.17	-0.20
AO	0.22	**0.46**	-0.06	-0.12	-0.06	0.18	0.23	0.02	0.14	-0.08
AO (Dec-Feb)	0.21	0.19	0.14	-0.02	0.10	-0.01	**0.33**	-0.26	-0.18	-0.16
QBO	-0.13	-0.07	-0.17	0.08	-0.16	0.22	0.16	0.21	-0.07	0.19
Gray Storm Count	-0.04	0.16	-0.13	-0.17	-0.09	-0.21	-0.17	-0.25	-0.13	0.11
Gray Hurricane Count	0.07	-0.08	0.10	0.20	0.03	0.23	0.07	**0.34**	0.08	0.06
Gray NTC	-0.04	-0.16	0.05	0.09	0.03	0.13	-0.02	0.23	-0.05	0.21
Global Average Temp.	0.21	0.23	0.08	0.09	-0.01	0.27	0.25	0.20	0.10	-0.01
NH Average Temp.	**0.31**	0.24	0.15	0.16	0.12	0.26	0.21	0.19	0.15	0.00
CO2 Radiative Forcing	0.14	0.25	0.12	-0.03	-0.17	0.20	**0.32**	0.13	-0.03	-0.14
Lean Solar Forcing	0.01	-0.17	0.02	0.18	0.13	0.00	0.01	-0.11	0.06	0.02
Sunspot Number	-0.20	-0.28	-0.14	0.01	0.10	-0.26	-0.11	**-0.34**	-0.09	-0.09

Influences on Temperature: 1953 to 1994

The correlation pattern when examined over the 1953 to 1994 subset of the temperature series (Table 7) is generally similar to that for the full record, but the correlations are mostly lower and fewer relationships are significant. The ENSO relationship is much less pronounced—the only significant relationship is to the NINO1+2 SST. The NAO and AO relationships, however, are more pronounced. This reflects the observation by Hurrell (1996) that the NAO and AO have undergone recent changes, increasing temperatures in North America. The relationship with the PNA remains about as important as in the full period of record. The relationships to global and hemispheric temperature are similar but weaker. Only one relationship (Northern Hemisphere average temperature to same-year average temperature) remains significant. CO_2 forcing on wintertime temperature increases in importance, while solar forcing is less prominent. Interestingly, a significant relationship appears with the sunspot number, perhaps reflecting the larger magnitude of sunspot fluctuations in recent cycles.

Precipitation

Means and Variability

Table 8 shows the basic statistical parameters for the 1867 to 1999 precipitation record for Hays. The minimum monthly total precipitation occurs in January and the maximum monthly total precipitation occurs in June. The range of precipitation through the year is very great, as June average precipitation is roughly 8 times January average precipitation. Similar to temperature, the increase in monthly precipitation through the first half of the year is more rapid than the decrease in the second half.

The variability of precipitation in Hays in an absolute sense is greater in the summer than the winter, but this is an artifact of the much greater amount of precipitation in summer. The coefficient of variation is, thus, a more useful value for analyzing precipitation. On this relative basis,

TABLE 8
Overall statistical parameters for the Hays precipitation time series (1867 to 1999) on monthly and annual bases.

Parameter	JAN	FEB	MAR	APR	MAY	JUN	JUL	AUG	SEP	OCT	NOV	DEC	TOT
Average (in)	0.46	0.74	1.22	2.13	3.32	3.52	3.32	2.93	2.20	1.41	0.88	0.65	22.78
Std. Dev.(in)	0.52	0.75	1.34	1.39	1.95	2.36	2.18	1.66	1.72	1.17	0.95	0.70	5.70
Coeff. of Variation	1.12	1.01	1.10	0.65	0.59	0.67	0.66	0.57	0.78	0.83	1.09	1.07	0.25
Min.(in)	0.00	0.00	0.00	0.05	0.15	0.17	0.01	0.00	0.06	0.00	0.00	0.00	9.21
Max. (in)	2.92	4.20	7.92	7.92	10.42	13.13	11.57	7.38	8.54	5.25	3.76	3.94	43.34
Range(in)	2.92	4.20	7.92	7.87	10.27	12.96	11.56	7.38	8.48	5.25	3.76	3.94	34.13

precipitation is much more temporally variable than temperature. While the standard deviation of annual average temperature is about 3% of the mean value, the standard deviation for average total annual precipitation is about 25% of the mean. For individual months, the variability is even greater (for example, in January the standard deviation of precipitation is 112% of the mean). Using the coefficient of variation, the winter months are clearly much more variable than the summer months. An examination of the minimum values shows that for seven of the twelve months, there are recorded instances of no precipitation at all.

Time Series Analysis

Extremes: Table 9 shows the twenty wettest years and twenty driest years during the period of record. The flood years of 1951 and 1993 were the wettest years ever recorded in Hays. The most extreme decade, however, was the 1870s, which contained four of the twenty wettest years (which is abnormally wet at the 90% significance level). The driest year ever recorded

TABLE 9
The 20 wettest and 20 driest years in Hays during the 1867 to 1999 period.

The 20 Wettest Years		The 20 Driest Years	
Year	Total annual precipitation (in. water equivalent)	Year	Total annual precipitation (in. water equivalent)
1951	43.34	1956	9.21
1993	37.99	1894	11.80
1878	35.40	1895	12.64
1973	35.00	1952	13.39
1902	34.43	1988	14.28
1915	34.14	1924	14.51
1903	32.52	1890	15.17
1875	32.08	1974	15.23
1996	31.78	1882	15.28
1932	31.66	1868	15.52
1898	31.24	1939	15.85
1958	31.21	1936	15.90
1877	30.21	1983	15.98
1928	29.94	1991	15.99
1944	29.70	1916	16.01
1942	29.61	1934	16.06
1886	28.74	1910	16.17
1876	28.64	1943	16.19
1992	28.53	1994	16.24
1957	28.33	1933	16.26

in Hays was 1956, with 1952 the fourth driest. It is worth noting that the 1930s Dust Bowl drought period contains none of the 10 driest years, but 4 of the years appear in the 20 driest (again, abnormally dry at the 90% significance level). The exceptional character of the 1930s, however, can be appreciated by considering that the years were among the warmest and the driest on record. While the 1950s drought was related almost entirely to a lack of precipitation, the Dust Bowl was a due to a combination of both. The 1890s was also a dry period in Hays, with 3 of the years in that decade appearing in the 10 driest years. These observations are illustrated in Figure 10, which shows the 1870s, 1900s, and 1940s as wet periods and the 1890s, 1910s, 1930s, and 1980s as relatively dry periods.

Trends: The regression of total annual precipitation against time over the period of record (Figure 11) shows no significant trend. The overall change over the 132 years has been a decrease of about 0.1 inch, which is

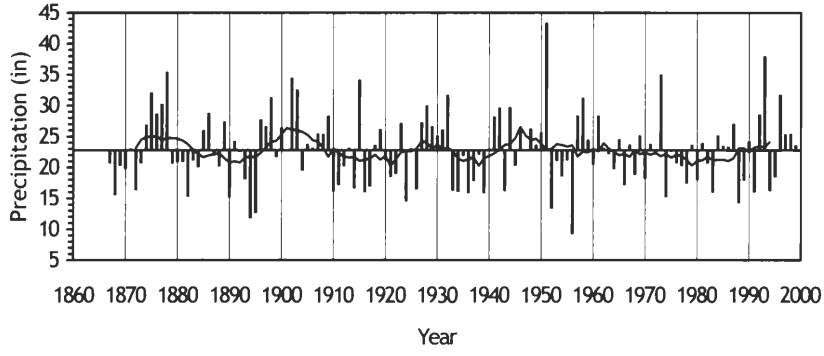

Figure 10. Annual total precipitation in Hays from 1867 to 1999 referenced to the long-term mean annual total precipitation (bars) and 11-year moving average (solid line).

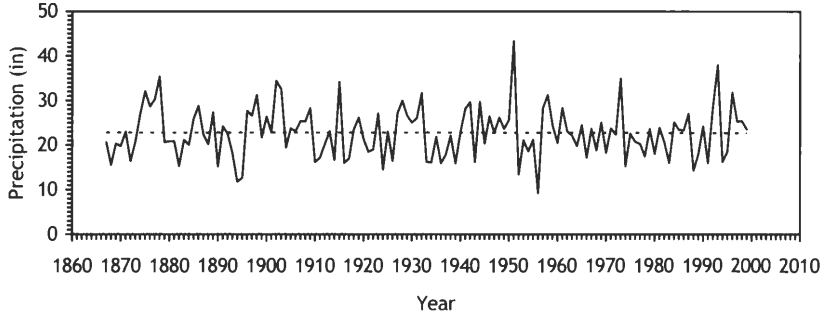

Figure 11. Annual total precipitation in Hays from 1867 to 1999 (solid line) and fitted regression line (dashed line).

not significant at the 95% level. The correlation of precipitation with time was found to be zero.

The analysis of precipitation trends by month (Table 10) shows that only two months (February and March) show a significant trend over the period of record. February precipitation has decreased, while March precipitation has increased. Both trends are very small, and explain only slightly more than 3% of the variance of precipitation in those months.

Periodicity: The autocorrelation analysis (Figure 12) shows that the most important correlation of the precipitation time series with itself is a negative correlation with a lag of 37 years. The second most important autocorrelation, also a negative one, has a lag of 5 years, perhaps representing one half of the 11-year solar cycle. Another negative autocorrelation exists at 8 years, and the lags of 5, 7, 8, and 9 years all have negative correlations. Important positive autocorrelations occur at lags of 42, 22, and 84 years. Of great interest are the small autocorrelations at lags of 1–4 years, implying that precipitation has very little persistence in Hays (i.e., that in any given year the precipitation is neither like nor unlike that in the previous 4 years).

The results of the spectral analysis of the Hays precipitation time series are shown in Figure 13. The most important periodicities are at wavelengths of 3.5 years, 2 years, 11 years, and about 23 years. The 3.5-year peak, by far the most important, is suggestive evidence of a strong relation between precipitation and the ENSO cycle. The 2-year peak is most likely related to the very low persistence of year-to-year temperature. The 11-year peak

TABLE 10
Trend analysis for Hays precipitation 1867 to 1999.
None of the trends are significant at the 95% level.

Month	Trend (in/yr)	R	R2
JAN	-0.1512	-0.1118	0.0125
FEB	-0.3453	-0.1776	0.0315
MAR	0.6339	0.1823	0.0332
APR	-0.3056	-0.0846	0.0072
MAY	-0.0832	-0.0164	0.0003
JUN	0.2333	0.0381	0.0015
JUL	0.3429	0.0606	0.0037
AUG	0.0956	0.0222	0.0005
SEP	-0.3761	-0.0847	0.0072
OCT	-0.1186	-0.0392	0.0015
NOV	0.3081	0.1244	0.0155
DEC	-0.3044	-0.1676	0.0281
TOT	-0.0723	-0.0049	0.0000

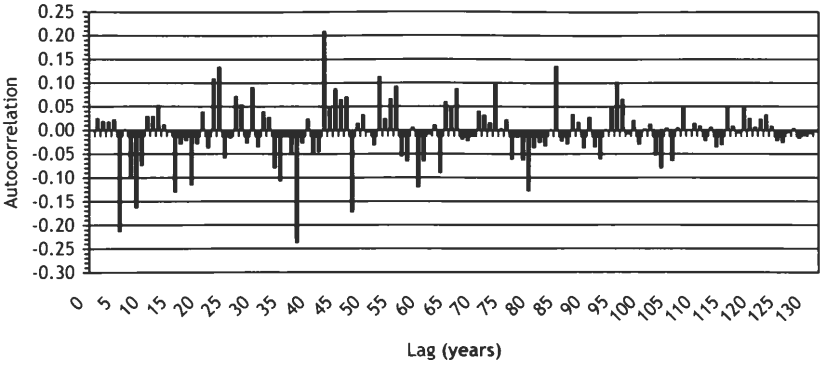

Figure 12. Autocorrelation analysis of the Hays annual total precipitation time series (1867 to 1999). The vertical axis shows the correlation of the time series with itself at the lag times given on the horizontal axis.

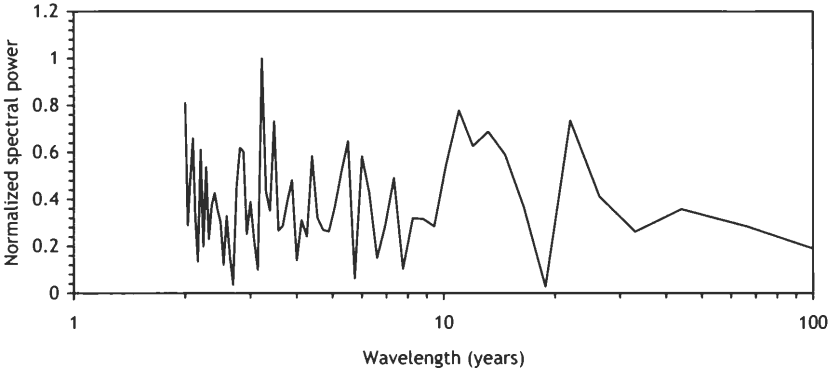

Figure 13. Spectral analysis of the Hays annual total precipitation time series (1867 to 1999). The curve represents the relative importance of pure sine wave components having the wavelengths on the horizontal axis.

may be related to the solar cycle, but it is much broader than that seen in the temperature analysis. The 23-year peak is interesting in view of the prominent positive autocorrelation with a lag of 23 years and may relate to the time between major floods in Hays. The folklore of Hays (J. Ratzlaff, personal communication) holds that floods occur in the city about every 20 years. The precipitation data shows that though this is not a strict rule, the gaps between floods are often around 20 to 24 years. Starting with 1907, there is a 20-year gap until the 1927 flood, then a 24-year gap until the 1951 flood. Skipping over the 1956 event, there is another 20-year gap until the 1970 flood, and then 23 years until the 1993 flood. Two possibilites exist to explain this periodicity—the 15–25-year cycle of the PDO (Minobe, 1997) and the 20–24-year Hale solar cycle (Perry, 1994).

TABLE 11

Analysis of possible influences on Hays precipitation during the full periods of record. Figures given are the correlation coefficients. Boldface figures indicate relationships significant at the 95% level. Unless otherwise noted, the variable is averaged over the entire year. For influences that cross the end of the year, the same-year values are for the year in which the earlier part of the averaging period falls.

	Correlation to Same-Year Precipitation					Correlation to Next-Year Precipitation				
Variable	**Annual**	**JFM**	**AMJ**	**JAS**	**OND**	**Annual**	**JFM**	**AMJ**	**JAS**	**OND**
SOI (Jun-Nov)	-0.10	-0.03	-0.07	0.02	**-0.19**	-0.11	**-0.18**	-0.07	0.03	-0.09
SOI (Dec-Feb)	0.03	0.01	0.09	0.05	**-0.19**	**-0.20**	**-0.25**	-0.11	0.00	**-0.19**
NINO1+2 (Jun-Nov)	0.19	0.17	0.09	0.07	0.20	0.03	**0.33**	-0.16	-0.04	0.18
NINO1+2 (Dec-Feb)	0.05	-0.02	0.02	0.00	0.19	0.11	**0.43**	-0.17	0.04	0.17
NINO3 (Jun-Nov)	0.18	0.12	0.08	0.12	0.12	0.02	**0.31**	-0.20	0.00	0.13
NINO3 (Dec-Feb)	0.07	-0.02	0.02	0.07	0.10	0.07	**0.43**	-0.15	-0.01	0.08
NINO4 (Jun-Nov)	0.19	0.16	0.05	0.17	0.04	-0.03	0.26	-0.26	0.01	0.12
NINO4 (Dec-Feb)	0.07	0.03	0.03	0.07	0.03	0.06	0.35	-0.17	0.05	0.07
Eq. Wind (Jun-Nov)	0.20	0.08	0.12	0.23	-0.07	0.06	**0.31**	-0.19	0.10	0.06
Eq. Wind (Dec-Feb)	0.07	0.01	0.07	0.04	0.03	0.16	**0.40**	-0.11	0.19	-0.05
PNA	0.05	0.25	-0.16	0.06	0.09	0.08	0.01	0.09	0.05	-0.02
PNA (Nov-Feb)	-0.06	0.02	-0.21	0.12	-0.07	0.00	0.12	-0.05	0.00	-0.02
PDO	0.13	**0.20**	0.04	0.02	0.15	0.06	0.11	-0.01	0.01	0.11
NAO	-0.13	-0.15	0.03	**-0.24**	0.12	-0.01	0.11	0.01	-0.03	-0.10
NAO (Dec-Feb)	0.03	0.13	0.02	-0.08	0.09	0.03	-0.01	0.13	-0.11	0.06
AO	-0.07	-0.04	-0.01	-0.07	-0.02	0.00	0.13	-0.04	0.00	-0.06
AO (Dec-Feb)	-0.04	0.11	-0.05	-0.05	-0.06	0.08	0.10	0.02	0.08	-0.01
QBO	0.17	0.11	0.12	0.14	-0.08	-0.17	-0.10	-0.12	-0.09	-0.06
Gray Storm Count	0.05	-0.09	0.19	-0.01	-0.09	-0.01	**-0.33**	0.25	-0.02	-0.16
Gray Hurricane Count	0.13	-0.17	0.25	0.15	-0.20	0.00	**-0.31**	0.28	-0.03	-0.19
Gray NTC	0.10	-0.17	0.21	0.17	-0.24	0.14	**-0.30**	**0.35**	0.18	-0.29
Global Average Temp.	0.09	0.14	0.01	0.06	0.01	0.00	0.07	-0.02	0.01	-0.05
NH Average Temp.	0.09	0.14	0.00	0.08	0.03	0.01	0.07	-0.03	0.03	-0.06
CO2 Radiative Forcing	-0.01	0.08	-0.07	0.00	0.02	-0.02	0.08	-0.07	-0.01	0.00
Lean Solar Forcing	-0.07	0.10	-0.08	-0.04	-0.12	0.00	0.13	-0.03	-0.01	-0.08
Sunspot Number	-0.10	0.02	-0.08	-0.07	-0.09	0.04	0.10	0.01	0.00	0.01

Influences on Precipitation: 1867 to 1999

Using the full 1867 to 1999 time series, a complex pattern of relationships (Table 11) between some of the factors and precipitation was found.

ENSO: Clearly, the ENSO cycle is important to precipitation. Both SOI measures have a moderately strong negative relationship to same-year autumn precipitation, indicating that during an El Niño event (when the SOI is negative), precipitation is higher. The SST variables all show a similar but stronger positive relationship to winter precipitation in the year after an El Niño, with the December to February SST having higher correlations than the June to November SST. The equatorial wind variable has a similar relationship to wintertime precipitation in the following year. The correlation of Pacific SST is highest for the NINO1+2 region and least for the NINO 4 region, so the condition of the waters closest to South America is most important for Hays precipitation. In general, the December to February measure of the ENSO cycle is superior to the November to June measure for elucidating the relationships. Table 12 shows the seasonal and annual average total precipitation values for the El Niño years as defined in the Quinn and de Mayolo (1987) dataset. The El Niño years and the succeeding years are quite a bit wetter than the long-term average, by about 1.2 inches. This increase in precipitation is greatest in summer and autumn in the El Niño year, and in winter for the year after the El Niño. However, as with temperature, none of these means are different from the long-term mean of all years at the 95% significance level.

PNA: The PNA shows no significant relationship to Hays precipitation.

PDO: The PDO shows a weak, but significant positive relationship to same-year springtime precipitation.

NAO, AO, and QBO: The NAO exhibits a moderate negative relationship to the same year summer precipitation. No significant relationships exist between the AO or QBO and Hays precipitation.

Atlantic tropical storms: The three tropical cyclone activities show moderate to strong negative relationships to winter precipitation and positive relationships to spring precipitation in the following year (i.e., a year with many tropical storms and hurricanes is likely to be succeeded by a dry winter and wet spring). Because of the long lead time, this relationship is a useful predictor for the Hays climate.

Table 12
Average annual and seasonal total precipitation for all years, El Niño years, and the years following El Niño years.

	Average Total Precipitation (in.)				
Years	JFM	AMJ	JAS	OND	Annual
All years	2.43	8.97	8.44	2.94	22.78
El Niño	2.58	8.69	9.36	3.27	23.90
El Niño + 1	2.83	8.99	8.83	3.32	23.97

Solar forcing: No significant relationships exist between the solar flux or sunspot data and Hays precipitation in the same or following years. However, solar output does exert an influence on Hays precipitation. Figure 14 shows the correlation between the annual difference of sunspot activity and annual precipitation with lags of 0 to 7 years. The greatest correlation (0.38) exists with a lag of 5 years, and this correlation is significant at the 95% level. This confirms the observation by Perry et al. (1994) of a 5-year lag between solar forcing and precipitation in the Midwest and could be used as a very long lead time predictor of climate. The correlation of the lagged solar forcing with precipitation is greater than that for the PDO, suggesting that the 20–24-year precipitation/flood periodicity discussed above is associated more with solar activity than the PDO.

Influences on Precipitation: 1953 to 1994

The pattern of correlation over the shorter 1953 to 1994 time period (Table 13) is generally similar to that over the full period, but some interesting differences appear. Some relationships are greater or more apparent, while others are weaker or less apparent.

ENSO: The relationship of winter precipitation to the ENSO cycle is even more pronounced over this period. The correlations of Pacific SST with Hays winter precipitation are larger, reaching 0.48 for the NINO1+2 region (meaning that about 23% of the variance of wintertime precipitation in Hays can be explained by the conditions in the eastern Pacific ocean). The equatorial wind index also shows a more pronounced relationship to winter precipitation, and for the shorter analysis period the equatorial winds show a significant relationship to the precipitation over the entire year. The exception to this is that the relationship with the SOI, which was

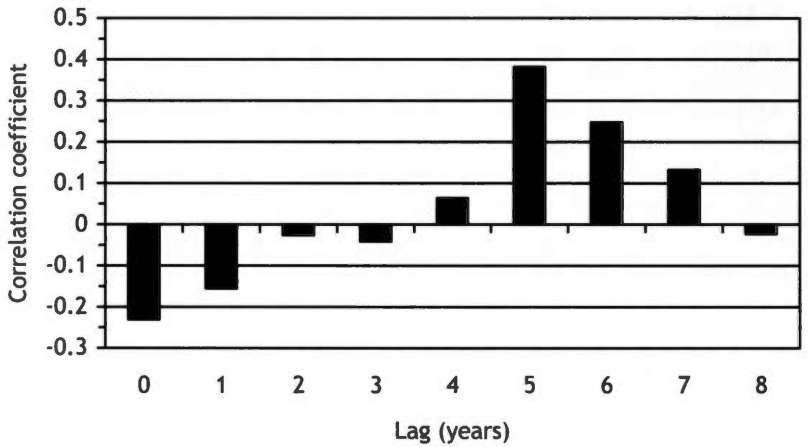

Figure 14. Correlation of annual sunspot number difference and Hays precipitation vs. lag time in years.

TABLE 13

Analysis of possible influences on Hays precipitation during the period 1953 to 1994. Figures given are the correlation coefficients. Boldface figures indicate relationships significant at the 95% level. Unless otherwise noted, the variable is averaged over the entire year. For influences that cross the end of the year, the same year values are for the year in which the earlier part of the averaging period falls.

	Correlation to Same-Year Precipitation					Correlation to Next-Year Precipitation				
Variable	Annual	JFM	AMJ	JAS	OND	Annual	JFM	AMJ	JAS	OND
SOI (Jun-Nov)	-0.21	-0.13	-0.07	-0.19	0.02	-0.10	-0.24	0.16	-0.09	-0.11
SOI (Dec-Feb)	0.01	0.00	-0.01	0.02	0.00	-0.25	**-0.38**	-0.02	-0.06	-0.19
NINO1+2 (Jun-Nov)	0.09	0.24	-0.05	-0.04	0.18	0.17	**0.35**	-0.05	0.02	0.19
NINO1+2 (Dec-Feb)	0.03	0.09	0.02	-0.09	0.15	0.18	**0.47**	-0.21	0.08	0.17
NINO3 (Jun-Nov)	0.14	0.20	0.00	0.06	0.08	0.13	**0.33**	-0.13	0.06	0.11
NINO3 (Dec-Feb)	0.07	0.06	0.00	0.04	0.06	0.16	**0.44**	-0.12	0.04	0.08
NINO4 (Jun-Nov)	0.28	0.22	0.05	0.25	0.02	0.17	0.31	-0.14	0.14	0.13
NINO4 (Dec-Feb)	0.14	0.09	0.04	0.13	0.01	0.26	**0.40**	-0.04	0.16	0.08
Eq. Wind (Jun-Nov)	0.23	0.07	0.09	0.27	-0.08	0.19	**0.34**	-0.13	0.17	0.05
Eq. Wind (Dec-Feb)	0.09	0.00	0.07	0.08	0.01	0.30	**0.42**	-0.01	0.24	-0.05
PNA	0.13	**0.35**	-0.22	0.11	0.13	0.09	0.04	0.20	0.00	-0.09
PNA (Nov-Feb)	0.09	0.16	-0.05	0.15	-0.14	0.02	0.12	-0.05	0.01	-0.03
PDO	0.27	**0.43**	0.02	0.05	0.20	0.12	0.27	0.01	-0.02	0.10
NAO	-0.03	-0.11	0.09	-0.14	0.19	0.13	0.25	0.04	0.01	0.00
NAO (Dec-Feb)	-0.06	0.27	-0.26	-0.14	0.21	0.20	0.05	0.22	0.02	0.20
AO	0.05	-0.09	0.11	0.01	0.07	0.06	0.16	-0.08	0.02	0.06
AO (Dec-Feb)	-0.16	0.07	-0.24	-0.14	0.07	0.28	0.14	0.14	0.19	0.13
QBO	0.24	0.11	0.13	0.20	-0.02	-0.22	-0.13	-0.12	-0.13	-0.11
Gray Storm Count	0.09	0.10	-0.05	0.10	0.02	0.30	0.10	0.12	0.24	0.17
Gray Hurricane Count	0.00	-0.18	0.12	0.10	-0.19	**-0.36**	**-0.39**	0.06	-0.23	-0.31
Gray NTC	0.00	-0.17	0.11	0.13	-0.27	-0.26	**-0.40**	0.07	-0.02	**-0.46**
Global Average Temp.	0.26	**0.40**	-0.15	0.24	0.08	-0.02	0.16	-0.14	-0.08	0.16
NH Average Temp.	0.20	0.28	-0.15	0.26	-0.03	-0.10	0.03	-0.11	-0.11	0.05
CO2 Radiative Forcing	0.08	0.29	-0.09	-0.06	0.18	0.08	0.30	-0.12	-0.05	0.22
Lean Solar Forcing	-0.04	0.24	-0.19	0.00	-0.13	0.20	0.26	-0.01	0.12	0.06
Sunspot Number	-0.05	0.14	-0.09	-0.06	-0.05	0.26	0.25	0.09	0.07	0.25

only moderate over the full period, disappears during the shorter period. The enhanced relationship to ENSO is perhaps related to the stronger El Niño events that have occurred in the last 30 years.

PNA: During the full period of record, no significant relationships was observed to exist between the PNA and Hays precipitation. However, a moderate relationship is evident in the shorter record between the annual average PNA index and same-year precipitation.

PDO: No significant relationship was observed between the PDO and Hays precipitation over the full period, but a strong relationship exists between the annual average PDO and same-year wintertime precipitation over the shorter period. This may reflect the observation by Mantua et al. (1997) that the circulation of the Pacific ocean has changed over the past few decades.

NAO, AO, and QBO: No significant relationships existed between any of these teleconnections and Hays precipitation over this period.

Tropical cyclones: The negative relationship of tropical storm frequency to following-year winter precipitation is stronger than during the full period of record, and the positive relationship to spring precipitation observed over the full record is not evident. The relationship to the annual total precipitation is also greater (and significant in the case of hurricane count) in the shorter period. This may be related to the increasing frequency of hurricanes over the past few decades (Landsea, 1993).

Global climate change and solar forcing: A significant positive relationship exists between the global average temperature and the same-year wintertime precipitation over the 1953 to 1994 period. This relationship does not exist with the Northern Hemisphere average temperature. Also, solar forcing and CO_2 radiative forcing, while not significant, show increased correlations compared with the full period analysis.

Summary and Conclusions

Summary of Results

In this study, the temperature and precipitation records of Hays were analyzed to identify the long-term mean state, variability, periodicity, and trends of Hays climate as well as to identify those regional and global processes that influence Hays climate. The more important results are listed below.

- Temperature in Hays is most variable in winter.
- Hays temperature has a strong year-to-year persistence.
- The warmest decade in the Hays temperature record was the 1930s, and the 1990s were almost as extreme.
- Temperature in Hays shows a substantial increase (of about 1.7 °F or 0.015 °F/yr) over the last 114 years. The increase has been greatest in March, June, July, and October.
- The rate of temperature increase over the last 30 years (about 0.057 °F/yr) has been almost 4 times as fast as the overall rate of increase.
- There are three distinct periods of change in Hays temperature, and these combined exhibit the strongest source of variability in the temperature record.
- Temperature in Hays is strongly coupled to global and hemispheric temperature, which also have been rising.

- The increase in Hays temperature is partly associated with changes in the CO_2 content of the atmosphere and partly with changes in solar activity.
- The eleven-year solar cycle is the second most important source of periodic variability in the Hays temperature record.
- Hays temperature has a clear relationship to the NAO and AO teleconnections, and this relationship has been more prominent recently. The NAO and AO have their greatest impact in wintertime. Stronger Icelandic Lows are associated with warmer temperatures in Hays.
- The ENSO cycle has connections to Hays temperature, but some of the observed relationships may be an artifacts of rising global ocean temperature.
- Volcanic eruptions as a whole have had no measurable effect on temperature in Hays.
- Hays precipitation is much more variable than temperature.
- The amount of precipitation in Hays is most variable during the summer. However, during the winter months, Hays receives substantially less precipitation, so variability relative to the mean is greater during winter.
- Precipitation shows very little year-to-year persistence.
- The driest period in the Hays precipitation record was during the 1950s drought.
- The Dust Bowl drought was driven by a combination of high temperatures and lower precipitation, with temperature being a more important factor.
- No significant trend exists in precipitation in Hays over the past 132 years.
- The greatest identifiable source of variability in Hays precipitation is the ENSO. ENSO is most influential on wintertime precipitation. The warm (El Niño) phase of the ENSO is associated with higher precipitation in Hays.
- A 22–23-year cycle exists in Hays precipitation, possibly related to a 20–24-year solar cycle.
- A strong relationship exists between tropical cyclone activity and precipitation in the following year.
- Precipitation in Hays is significantly related to the change in solar flux with a 5-year lag.

Utility

How can people make direct use of the results of this study? Scientists in fields ranging from geology to agriculture can use the long-term statistics on temperature and precipitation as well as the influence analysis to determine the way climate affects their subject areas. Agricultural producers can use the seasonal cycle information to help make planting and harvesting decisions, and they can use the analysis of climate influences to help reduce risk by making rationally-based estimates of future precipitation. Emergency-management professionals can gain advance warning of the possibility of droughts and floods by examining regional and global circulation patterns. Water-supply developers and managers can use the long-term statistics to help establish the inputs into the hydrologic system, and they can use the data on precipitation extremes and temperature trends to assess future changes in hydrologic inputs and demands on water resources. Historians can use the time-series analysis to understand the effects of climate on migration, development, and disease. Finally, curious residents can use the study to help answer questions like "When will the summer finally end?" or "Why is it raining so much this spring?"

Future Work

The work presented here, while definitive in some areas, can and will be extended in the future. Particular areas for future research include (1) expanding the study area to include the entire Kansas High Plains, (2) relating the observed Hays climate trends to the predictions of global and regional climate system models, (3) relating the climate influences to variables of direct importance to quality of life, such as crop yields, water supply usage, and aquifer depletion, and (4) relating the climate influences to the frequency and magnitude of extreme weather events, such as thunderstorms, lightning, hail, tornadoes, and blizzards. No attempt was made in this study to develop a quantitative predictive capability for the climate of Hays based on the observed trends and relationships. Such an effort is a natural successor to this study, and some of the relationships (e.g., NAO and temperature, ENSO and precipitation, Atlantic tropical storms and precipitation, solar forcing and both temperature and precipitation) offer the possibility of successful climate prediction several seasons in advance. A major challenge to developing a predictive equation for climate lies in the physical connections and collinearities between many of the forcing factors.

Acknowledgements

I wish to gratefully acknowledge the assistance of Dr. John Ratzlaff of FHSU, who offered valuable suggestions during the preliminary phases of this research. I would also like to thank the various data centers that provided the data for this study, including JISAO, NGDC, NOAA CMDL, NOAA AOML, the University of East Anglia, the NOAA Climate Prediction Center, and the Kansas State Climatologist's Office. The data processing and analysis in this study were conducted using the Interactive Data Language (IDL) and Microsoft Excel. The maps were made using Geocart and annotated with Adobe Illustrator.

References

Abawi, G. Y., R. J. Smith, and D. K. Brady, 1995, Assessment of the value of long range weather forecasts in wheat harvest management, *J. Agric. Eng.*, 62, 39–48.

Adams, R. M., K. J. Bryant, B. A. McCarl, D. M. Legler, J. J. O'Brien, A. R. Solow, and R. Weiher, 1995, Value of improved long-range weather information, *Contemporary Economic Policy*, 13, 10–19.

Allan, R. J., N. Nicholls, P. D. Jones, and I. J. Butterworth, 1991, A further extension of the Tahiti-Darwin SOI, early SOI results and Darwin pressure, *J. Climate*, 4, 743–49.

Allen, C. W., 1973, *Astrophysical Quantities*, Athlone Press, London.

Anderson, B. R., 1975, *Weather in the West*, American West Publishing Company, Palo Alto, California.

Barnston, A. G., and R. E. Livezey, 1987, Classification, seasonality and persistence of low-frequency atmospheric circulation patterns, *Mon. Wea. Rev.*, 115, 1083–126.

Barry, R. G., and R. J. Chorley, 1987, *Atmosphere. Weather, and Climate (5th ed.)*, Methuen and Co., London.

Bell, G. D., and J. E. Janowiak, 1995, Atmospheric circulation associated with the Midwest floods of 1993, *Bull. Amer. Met. Soc.*, 5, 681–95.

Bove, M. C., 1998, Impacts of ENSO on United States tornadic activity, *Preprints, 9th Conference on Global Change Studies*, Phoenix, AZ, Amer. Meteor. Soc., 199–202.

Bove, M. C., J. B. Elsner, C. W. Landsea, X. Niu, and J. J. O'Brien, 1998, Effects of El Niño on U.S. landfalling hurricanes, revisited. *Bull. of the Amer. Met. Soc.*, 79, 2477–82.

Chagnon, S. A., 1996, *The Great Midwest Flood of 1993*, Westview Press, Boulder, CO.

Crowley, T. J. , 2000, Causes of climate change over the Past 1000 years, *Science*, 289: 270–77.

Eddy, J.,1976, *The Maunder Minimum*, Science, 192, 1189–202.

Gray, W. M., C. W. Landsea, P. W. Mielke, and K. J. Berry, 1994, Predicting Atlantic Basin seasonal tropical cyclone activity by 1 June, *Weather and Forecasting*, Vol. 9, 103–15.

Gray, W. M., J. D. Sheaffer, and J. A. Knaff, 1992, Influence of the stratospheric QBO on ENSO variability, *J. Meteor. Soc. Japan*, 70, 975–95.

Hansen, J., M. Sato, and R. Ruedy, Radiative forcing and climate response, *J. Geophys. Res.*, 102, 6831–64, 1997.

Hays Daily News (HDN), *Hays 1900-1999, A Look Back*, October 13, 1999.

Horel, J. D., and J.M. Wallace, 1981, Planetary scale atmospheric phenomena associated with the Southern Oscillation, *Mon. Wea. Rev.*, 109, 813–29.

Hurd, B., N. Leary, R. Jones, and J. Smith, 1999, Relative regional vulnerability of water resources to climate change, *J. Am. Water Resources Assn.*, 35(6), 1399–410.

Hurrell, J. W., 1995, Decadal trends in the North Atlantic Oscillation: Regional temperatures and precipitation. *Science*, 269, 676–79.

Hurrell, J. W., 1996, Influence of variations in extratropical wintertime teleconnections on Northern Hemisphere temperatures, *Geophys. Res. Lett.*, 23, 665–68.

Hurrell, J. W., and H. van Loon, 1997, Decadal variations in climate associated with the North Atlantic oscillation, *Clim. Change*, 36, 301–26.

Intergovernmental Panel on Climate Change (IPCC), 1995, *Climate Change 1995 – The IPCC Second Assessment*, J. T. Houghton, L. G. Meira Filho, B. A. Callender, N. Harris, A. Kattenberg and K. Maskell (Eds.), Cambridge University Press, Cambridge, United Kingdom.

Intergovernmental Panel on Climate Change (IPCC), 1997, *The Regional Impacts of Climate Change: An Assessment of Vulnerability*, R. T. Watson, M. C. Zinyowera, R. H. Moss (Eds), Cambridge University Press, Cambridge, United Kingdom.

Jones, P. D., 1994a, Recent warming in global temperature series, *Geophys. Res. Lett.*, 21, 1149–52.

Jones, P. D., 1994b, Hemispheric surface air temperature variations: A reanalysis and an update to 1993, *J. Climate*, 7, 1794–802.

Jones, P. D., T. Jónsson, and D. Wheeler, 1997, Extension to the North Atlantic Oscillation using early instrumental pressure observations from Gibraltar and South-West Iceland, *Int. J. Climatol.*, 17, 1433–50.

Jones, P. D., Osborn, T. J., and Briffa, K.R., 1997, Estimating sampling errors in large-scale temperature averages, *J. Climate*, 10, 2548–68.

Jones, P. D., S. C. Raper, R. S. Bradley, H. F. Diaz, P. M. Kelly, and T. M. L. Wigley, 1986, Northern Hemisphere surface air temperature variations: 1851-1984, *J. Clim. Appl. Met.*, 25, 161–79.

Kansas Water Office, 1999, *Kansas Reported Water Use Summary*, Division of Water Resources, Topeka, Kansas.

Körner, T. W., 1989, *Fourier Analysis*, Cambridge University Press, Cambridge.

Landsea, C. W., 1993, A climatology of intense (or major) Atlantic hurricanes, *Mon. Wea. Rev.*, 121, 1703–13.

Lassen, K., and E. Friis-Christensen, 1995, Variability of the solar cycle length during the past five centuries and the apparent association with terrestrial climate, *J. Atm.Terr. Phys.*, 57, 835–45.

Lean, J., J. Beer, and R. Bradley, 1995, Reconstruction of solar irradiance since 1610: Implications for climate change, *Geophys. Res. Lett.*, 22 (23), 3195–98.

Leathers, D. J., and M. A. Palecki, 1992, The Pacific/North American teleconnection pattern and United States climate. Part II: Temporal characteristics and index specification, *J. Climate*, 5, 707–16.

Lettenmaier, D. P., D. Ford, J. P. Hughes, and B. Nijssen, 1996, *Water Management Implications of Global Warming: 5. The Missouri River Basin (Report to Interstate Commission on the Potomac River Basin and Institute for Water Resources, U.S. Army Corps of Engineers)*, DPL and Associates, Seattle, Washington.

Mantua, N. J., S. R. Hare, Y. Zhang, J.M. Wallace, and R.C. Francis, 1997, A Pacific interdecadal climate oscillation with impacts on salmon production, *Bull. Amer. Meteo. Soc.*, 78, pp. 1069–79.

Marquardt, C., and B. Naujokat, 1997: An update of the equatorial QBO and its variability, 1st SPARC Gen. Assemb., Melbourne Australia, *WMO/TD-No. 814*, Vol. 1, 87–90.

Maruyama, T., 1997, The quasi-biennial oscillation(QBO) and equatorial waves - a historical review, *Meteo. & Geophys.*, 48, 1–17.

Maruyama, T., and Y. Tsuneoka, 1988, Anomalously short duration of the easterly wind phase of the QBO at 50hPa in 1987 and its relationship to an El Niño event, *J. Meteor. Soc. Japan*, 66, 629–34.

Mauget, S.A., and D. R. Upchurch, 1999, El Niño and La Niña related climate and agricultural impacts over the Great Plains and Midwest, *J. of Production Agric.*, 12(2), 203–14.

McNab, A. L., and T. R. Karl, 1991, Climate and Droughts, in Paulson, R. W., E. B. Chase, R. S. Roberts, and D. W. Moody, compilers, National Water Summary 1988–89—Hydrologic Events and Floods and Droughts, *U. S. Geological Survey Water-Supply Paper 2375*, 89–98.

Minnis, P., E. F. Harrison, L. L. Stowe, G. G. Gibson, F. M. Denn, D. R. Doelling, and W. L. Smith, Jr., 1993, Radiative climate forcing by the Mount Pinatubo eruption, *Science*, 259, 1411–5.

Minobe, S., 1997, A 50-70 year climatic oscillation over the North Pacific and North America, *Geophys. Res. Lett.*, 24, 683–6.

Naujokat, B., 1986, An update of the observed quasi-biennial oscillation of the stratospheric winds over the tropics, *J. Atmos. Sci.*, 43, 1873–7.

Newhall, C. G., and S. Self, 1982, The volcanic explosivity index (VEI): An estimate of explosive magnitude for historical volcanism, *J. Geophys. Res.*, 87 (C2), 1231–8.

Ojima, D., L. Garcia, E. Elgaali, K. Miller, T. G. F. Kittel, and J. Lackett, 1999, Potential climate change impacts on water resources in the Great Plains, *J. Amer. Water Resources Assn.*, 35(6), 1443–53.

Olsen, J. R., J. R. Stedinger, N. C. Matalas, and E. Z. Stakhiv, 1999, Climate variability and flood frequency estimation for the Upper Mississippi and Lower Missouri Rivers, *J. Amer. Water Resources Assn.*, 35(6), 1509–23.

Owenby, J. R., and D. S. Ezell, 1992, *Monthly Station Normals of Temperature, Precipitation, and Heating and Cooling Degree Days, 1961-90, Kansas*, Climatography of the United States No. 81, NOAA National Climatic Data Center, Asheville, North Carolina.

Perry, C. A., 1994, Solar-irradiance variations and regional precipitation fluctuations in the western United States: *Intl. J. Climatol.*, 14, 969–83.

Perry, C. A., 1995, Association between solar-irradiance variations and hydroclimatology of selected regions of the USA, *Proceedings of the 6th International Meeting on Statistical Climatology*, June, 1995, Galway, Ireland, 239–42.

Quinn, W. H., 1992, A study of Southern Oscillation-related climatic activity for A. D. 622-1900 incorporating Nile River flood data, in *El Niño historical and paleoclimatic aspects of the Southern Oscillation*, H. F. Diaz and V. Markgraf, Eds., Cambridge University Press, 119–49.

Quinn, W. H., and S. E. A. de Mayolo, 1987, El Niño occurrences over the past four and-a-half centuries, *J. Geophys. Res.*, 92 (C13), 14,449–61.

Philander, S. G. H., 1990, *El Niño, La Niña, and the Southern Oscillation*, Academic Press, San Diego.

Redmond, K. T., and R. W. Koch, 1991, Surface climate and streamflow variability in the Western United States and their relationship to large-scale circulation indices, *Water Resources Research*, 27(9), 2381–99.

Reed, R. G., W. J. Campbell, L. A. Rasmussen, and D. G. Rogers, 1961, Evidence of downward-propagating annual wind reversal in the equatorial stratosphere. *J. Geophys. Res.*, 66, 813–8.

Rogers, J. C., and H. van Loon, 1979, The seesaw in winter temperatures between Greenland and northern Europe. Part II: Some oceanic and atmospheric effects in middle and high latitudes, *Mon. Wea. Rev.*, 107, 509–19.

Ropelewski, C. F., and P. D. Jones, 1987, An extension of the Tahiti-Darwin Southern Oscillation Index, *Mon. Wea. Rev.*, 115, 2161–5.

Shapiro, L. J., 1989, The relationship of the quasi-biennial oscillation to Atlantic tropical storm activity, *Mon. Wea. Rev.*, 117, 1545–52.

Shindell, D. T., R. L. Miller, G. A. Schidt, and L. Pandalfo, 1999, Simulation of recent northern winter climate trends by greenhouse-gas forcing, *Nature*, 399, 452–5.

Sigurdsson, H., 1982, Volcanic pollution and climate: The 1783 Laki eruption, *Eos*, 63 (32), 600–2.

Simarski, L. T., 1992, *Volcanism and climate change*, Special Report, American Geophysical Union, Washington, D. C.

Stommel, H., and E. Stommel, 1983, *Volcano Weather - The Story of the Year Without a Summer 1816*, Seven Seas Press, Newport, R. I.

Thompson, D. W., and J. M. Wallace, 1998, The Arctic Oscillation signature in the wintertime geopotential height and temperature fields, *Geophys. Res. Lett.*, 25 (9), 1297–300.

Trenberth, K., 1991, General haracteristics of El Niño-Southern Oscillation, in *Teleconnections Linking Worldwide Climate Anomalies*, M. Glantz, R. Katz, and N. Nicholls (Eds.), Cambridge University Press, Cambridge.

Trenberth, K. E., and J. W. Hurrell, 1994, Decadal atmosphere-ocean variations in the Pacific, *Clim. Dyn.*, 9, 303–14.

United States Department of Agriculture (USDA), 1997, *Census of Agriculture*, Washington, D. C.

United States Environmental Protection Agency (EPS), 1998, *Climate Change and Kansas*, EPA 236-F-0071, EPA Office of Policy, Washington, D. C., September 1988.

Walker, G. T., and E. W. Bliss, 1932, World Weather V, *Memoirs of the Royal Meteorological Society*, 4, 53–84.

Wallace, J. M., 2000, North Atlantic Oscillation/Nortthern Hemisphere Annular Mode: One phenomenon, two paradigms, *Quart. J. Royal Met. Soc.*, 126, 791–805.

Wallace, J. M., and D. S. Gutzler, 1981, Teleconnections in the geopotential height field during the Northern Hemisphere Winter, *Mon. Wea. Rev.*, 109, 784–812.

Webb, G., 1986, Solar physics and the origins of dendrochronology, *Isis*, 77, 292–301.

Weller, G., 1998, Regional impacts of climate change in the Arctic and Antarctic, *Annals of Glaciol.*, 27, 543–52.

Worster, D., 1979, *Dust Bowl: The Southern Plains in the 1930's*, Oxford University Press, Oxford.

Zhang, Y., J. M. Wallace, and D. S. Battisti, 1997, ENSO-like interdecadal variability: 1900-93, *J. Climate*, 10, 1004–20.

FORT HAYS STATE
UNIVERSITY

www.fhsu.edu